

Fast non-overlapping Schwarz domain decomposition methods for solving the neutron diffusion equation

Erell Jamelot^a, Patrick Ciarlet Jr^b

^a*Commissariat à l'Énergie Atomique et aux Énergies Alternatives, CEA Saclay, 91191 Gif-sur-Yvette Cedex, France*

^b*POEMS Laboratory, CNRS-INRIA-ENSTA UMR 7231, ENSTA ParisTech 32, Boulevard Victor, 75739 Paris Cedex 15, France*

Abstract

Studying numerically the steady state of a nuclear core reactor is expensive, in terms of memory storage and computational time. In order to address both requirements, one can use a domain decomposition method, implemented on a parallel computer. We present here such a method for the mixed neutron diffusion equations, discretized with Raviart-Thomas-Nédélec finite elements. This method is based on the Schwarz iterative algorithm with Robin interface conditions to handle communications. We analyse this method from the continuous point of view to the discrete point of view, and we give some numerical results in a realistic highly heterogeneous 3D configuration. Computations are carried out with the MINOS solver of the APOLLO3^{®1} neutronics code.

Keywords: nuclear core reactor, mixed neutron diffusion equations, Raviart-Thomas-Nédélec finite elements, domain decomposition methods, Robin interface conditions, Schwarz iterative method, fast solvers

Introduction

A nuclear reactor produces thermal energy, which is released from induced nuclear fission on fissile atoms, such as uranium. The fission produces kinetic energy, γ radiation, lighter atomic nuclei, and free neutrons. These neutrons may lead to other fissions: this process is known as the nuclear

¹APOLLO3 is a registered trademark in France.

chain reaction. In order to compute the power of a nuclear reactor, one studies the steady state of its core, which is the place where fission occurs.

The behaviour of a nuclear core reactor depends on the nuclear chain reaction, which is described by the neutron balance equation, or more simplified models. We refer to [11, 7] for a general description of nuclear core reactors. In practice, it is advised to implement fast numerical methods to reduce the overall computational cost. To that aim, we choose a discretization of an approximate model, the neutron diffusion equation, by well-known finite elements and use a domain decomposition method, suitable for high performance computing.

Note that domain decomposition methods are often used in core solvers. For instance, in [23, 1], a Schur complement method is used to accelerate the SP_N core solver developed at EDF (Electricité de France). In [38, 37], the Schwarz iterative algorithm with Robin interface conditions is applied to the P_N core solver PARAFISH. Whereas, in [39, 40], L. N. Zaslavsky proposes a multigrid solver, using the finite difference method for the diffusion equation. Finally, the *response matrix method*, [26, 32, 8] which implements a two-level model, helps reduce the computational time.

The diffusion approximation is widely studied for both physical and numerical reasons. From a physical point of view, it is well suited to model homogeneous core reactors. The multigroup diffusion equations are cheaper to solve than the neutron transport equation. Moreover, until recently, the two-group diffusion equations was the only way to compute the neutrons flux of the whole core reactor. From a numerical point of view, it leads to the introduction of the Simplified P_N equations (the so-called SP_N equations) which can be written as a coupled set of diffusion equations [30, 2, 3]. These equations can be further simplified, leading to the neutron diffusion equation. In this paper, we present a domain decomposition method used to accelerate the numerical solution of the mixed formulation of the neutron diffusion equation.

In the next part, we provide some physical background. In the second part, we detail the algorithm that has to be implemented to solve the model, and we define the problem from a mathematical point of view. In the third part, we study an equivalent variational formulation and its discretization. Then in the fourth part, we describe the non-overlapping Schwarz domain decomposition we implemented, and furthermore we prove its convergence under suitable assumptions. We detail its discretization in the fifth part: we show that the method corresponds to either a block Jacobi, or a block Gauss-Seidel

method. In the last part, we give some numerical results on a realistic highly heterogeneous 3D numerical experiment.

1. Background

For simplicity reasons, we will study in this paper the one-speed diffusion approximation. From this study, one can easily deduce the multigroup diffusion case [7, 11]. In the time independent case, the balance of the neutron flux is governed by these equations, where the 2-tuple $(\mathbf{p}(\mathbf{x}), \phi(\mathbf{x}))$ represents the neutron current and the neutron flux:

$$\begin{cases} \frac{1}{D} \mathbf{p} + \mathbf{grad} \phi = 0 \\ \text{div } \mathbf{p} + \Sigma_a \phi = \frac{1}{\lambda} \Sigma_f \phi \end{cases} \quad (1)$$

Above, if we let $\Sigma_t(\mathbf{x})$ be the total cross section and $\Sigma_s(\mathbf{x})$ the scattering cross section, then $\Sigma_a = \Sigma_t - \Sigma_s$ is the absorption cross section. On the other hand, the diffusion coefficient $D(\mathbf{x})$ can be derived in two ways:

- using the spherical harmonics:

$$D(\mathbf{x}) = \frac{1}{3(\Sigma_t(\mathbf{x}) - \bar{\mu}_0 \Sigma_s(\mathbf{x}))}, \quad (2)$$

where $\bar{\mu}_0$ is the average scattering angle cosine [11].

- Under some additional physical assumptions: ie. that the medium is homogeneous, the variations of the flux are small, and the spatial dependence of the flux is linear, computing the neutrons flux across a small surface yields Fick's law [7] with another coefficient:

$$D(\mathbf{x}) = \frac{1}{3 \Sigma_t(\mathbf{x})}. \quad (3)$$

Actually, it is better to choose (2), which is usually called the diffusion coefficient with transport correction. On the other hand, it is more costly, since one must compute $\bar{\mu}_0$.

Eqs. (1) can be reduced to a primal form, depending only on the neutron flux ϕ , which is governed by:

$$-\text{div} (D \mathbf{grad} \phi) + \Sigma_a \phi = \frac{1}{\lambda} \Sigma_f \phi. \quad (4)$$

Due to the structure of Eq. (4), we remark that Eqs. (1) actually correspond to an eigenproblem, where λ acts as the inverse of an eigenvalue, with associated eigenflux ϕ . One can apply the Krein-Rutman theorem [22] to problem (1): the physical solution is necessarily positive, and it is the eigenfunction associated to the largest eigenvalue $k_{eff} = \max_{\lambda} \lambda$, which is in addition simple. More precisely, k_{eff} characterizes the physical state of the core reactor:

- if $k_{eff} = 1$: the core reactor is in a steady state and the nuclear chain reaction is self-sustaining. The reactor is said to be *critical*;
- if $k_{eff} > 1$: there are more neutrons which are produced than neutrons which disappear. The chain reaction races. The reactor is said to be *supercritical*;
- if $k_{eff} < 1$: there are less neutrons which are produced than neutrons which disappear. The chain reaction vanishes. The reactor is said to be *subcritical*.

We consider from now on that the current \mathbf{p} is such that $\int_{\mathcal{R}} |\mathbf{p}|^2 d\mathbf{x} < \infty$.

Different conditions on the boundary can be taken into account, such as: zero flux: $\phi = 0$; reflection: $\mathbf{p} \cdot \mathbf{n} = 0$; albedo: $\mathbf{p} \cdot \mathbf{n} = \alpha \phi$, with $\alpha > 0$; vacuum: $\mathbf{p} \cdot \mathbf{n} = \frac{1}{2} \phi$. In terms of the flux ϕ , the first three conditions correspond respectively to:

- a *Dirichlet* boundary condition: $\phi = 0$;
- a *Neumann* boundary condition: $D \frac{\partial \phi}{\partial n} = 0$;
- a *Robin* boundary condition: $\left(D \frac{\partial \phi}{\partial n} + \alpha \phi \right) = 0$.

2. The neutron diffusion equation

2.1. Inverse power algorithm for the eigenvalue problem

As we look for the smallest eigenvalue k_{eff} of Equation (1), the solution $(\mathbf{p}, \phi, k_{eff})$ can be computed by the inverse power iteration algorithm. After some initial guess is provided, at iteration number $m + 1$, we deduce $(\mathbf{p}^{m+1}, \phi^{m+1}, k_{eff}^{m+1})$ from $(\mathbf{p}^m, \phi^m, k_{eff}^m)$ by solving Equations (1) with

a source term. Set in a domain \mathcal{R} , the inverse power iteration algorithm² reads (we choose zero flux boundary conditions on $\partial\mathcal{R}$):

Set $(\mathbf{p}^0, \phi^0, k_{eff}^0)$, $m = 0$.

Until convergence, do: $m \leftarrow m + 1$

Solve:

$$\begin{cases} \frac{1}{D} \mathbf{p}^{m+1} + \mathbf{grad} \phi^{m+1} = 0 \text{ in } \mathcal{R}, \\ \operatorname{div} \mathbf{p}^{m+1} + \Sigma_a \phi^{m+1} = \frac{1}{k_{eff}^m} \Sigma_f \phi^m \text{ in } \mathcal{R}, \\ \phi^{m+1} = 0 \text{ on } \partial\mathcal{R}. \end{cases} \quad (5)$$

$$\text{Compute: } k_{eff}^{m+1} = k_{eff}^m \frac{\int_{\mathcal{R}} (\Sigma_f \phi^{m+1})^2}{\int_{\mathcal{R}} (\Sigma_f \phi^{m+1} \Sigma_f \phi^m)}.$$

End

Above, the Eqs. (5) with unknowns $(\mathbf{p}^{m+1}, \phi^{m+1})$ model the so-called *source solver* (here, the right-hand side is a function of ϕ^m). The updated value k_{eff}^{m+1} is inferred as follows: assuming that $\operatorname{div} \mathbf{p}^{m+1} + \Sigma_a \phi^{m+1} = (k_{eff}^{m+1})^{-1} \Sigma_f \phi^{m+1}$, one can write $(k_{eff}^{m+1})^{-1} \Sigma_f \phi^{m+1} = (k_{eff}^m)^{-1} \Sigma_f \phi^m$ and, multiplying this equation by $\Sigma_f \phi^{m+1}$ and integrating over the domain of computation \mathcal{R} , we obtain the last equation of (5). The convergence criterion is usually set on $|k_{eff}^{m+1} - k_{eff}^m|$ and $\int_{\mathcal{R}} (\Sigma_f \phi^{m+1} - \Sigma_f \phi^m)^2$. The inverse power iterations are called the outer iterations in opposition to the inner iterations, which correspond to the iterations of the source solver. As a matter of fact, one can choose an iterative source solver. See Subsection 4.3 for a motivation of such a choice.

2.2. Setting of the problem

First, we consider equations (1), with a source term S_f , namely we focus on the linear system solver step of the above algorithm. We let \mathcal{R} be a bounded, connected and open subset of \mathbb{R}^d , $d = 1, 2, 3$, having a Lipschitz

²This algorithm is described as well in [1] (algorithm 1, p. 2007).

boundary $\partial\mathcal{R}$ which is piecewise smooth. We split the boundary into three disjoint, open parts such that: $\partial\mathcal{R} = \bar{\Gamma}_D \cup \bar{\Gamma}_N \cup \bar{\Gamma}_R$. The mixed neutrons diffusion equations read:

Find (\mathbf{p}, ϕ) such that:

$$\left\{ \begin{array}{ll} \frac{1}{D} \mathbf{p} + \mathbf{grad} \phi = 0 & \text{in } \mathcal{R}, \\ \operatorname{div} \mathbf{p} + \Sigma_a \phi = S_f & \text{in } \mathcal{R}, \\ \phi = 0 & \text{on } \Gamma_D, \\ \mathbf{p} \cdot \mathbf{n} = 0 & \text{on } \Gamma_N, \\ -\mathbf{p} \cdot \mathbf{n} + \alpha \phi = 0 & \text{on } \Gamma_R. \end{array} \right. \quad (6)$$

Let $L^\infty(\mathcal{R})$ be the space of measurable bounded functions, and $L^2(\mathcal{R})$ be the space of measurable and square integrable functions. We suppose that we satisfy the following assumptions on the data: $D \in L^\infty(\mathcal{R})$, with $0 < D_* < D < D^*$ almost everywhere, $\Sigma_a \in L^\infty(\mathcal{R})$ with $0 \leq \Sigma_a \leq (\Sigma_a)^*$ ae., $\alpha \in \mathbb{R}_+^*$, $S_f \in L^2(\mathcal{R})$. Note that the current \mathbf{p} is such that $\mathbf{p} \in L^2(\mathcal{R})^d$. We introduce the following Sobolev spaces:

$$H^m(\mathcal{R}) := \left\{ u \in L^2(\mathcal{R}) \mid \left(\sum_{|j| \leq m} \int_{\mathcal{R}} |\partial_{\mathbf{x}}^j u|^2 d\mathbf{x} \right)^{1/2} < \infty \right\} \quad (m \geq 0),$$

$$\mathbf{H}(\operatorname{div}, \mathcal{R}) := \{ \mathbf{q} \in L^2(\mathcal{R})^d \mid \operatorname{div} \mathbf{q} \in L^2(\mathcal{R}) \},$$

with norms ($L^2(\mathcal{R}) = H^0(\mathcal{R})$):

$$\|u\|_m := \left(\sum_{|j| \leq m} \int_{\mathcal{R}} |\partial_{\mathbf{x}}^j u|^2 d\mathbf{x} \right)^{1/2} \quad (m \geq 0), \quad \|\mathbf{q}\|_{\mathbf{H}(\operatorname{div}, \mathcal{R})} := (\|\mathbf{q}\|_0^2 + \|\operatorname{div} \mathbf{q}\|_0^2)^{1/2}.$$

We will need the semi-norms:

$$|u|_m := \left(\sum_{|j|=m} \int_{\mathcal{R}} |\partial_{\mathbf{x}}^j u|^2 d\mathbf{x} \right)^{1/2} \quad (m \geq 0).$$

We will need as well the H^s Sobolev spaces with $s = m + \sigma$, $m \in \mathbb{N}$ and $0 < \sigma < 1$: $H^s(\mathcal{R}) = \{u \in H^m(\mathcal{R}) \mid |u|_s < \infty\}$, where the semi-norm $|\cdot|_s$ is defined by:

$$|u|_s = \left(\sum_{|j|=m} \int_{\mathcal{R}} \int_{\mathcal{R}} \frac{|\partial_{\mathbf{x}}^j u(\mathbf{x}) - \partial_{\mathbf{x}}^j u(\mathbf{y})|^2}{|\mathbf{x} - \mathbf{y}|^{d+2\sigma}} d\mathbf{x} d\mathbf{y} \right)^{1/2}.$$

2.3. The primal neutron diffusion equation

Define $H_{0,\Gamma_D}^1(\mathcal{R}) := \{\psi \in H^1(\mathcal{R}) \mid \psi|_{\Gamma_D} = 0\}$. Recall that (\mathbf{p}, ϕ) is governed by (6): as $\mathbf{p} \in L^2(\mathcal{R})^d$, we deduce that $\phi \in H_{0,\Gamma_D}^1(\mathcal{R})$. Furthermore, we can rewrite equivalently equations (6) with the flux $\phi \in H_{0,\Gamma_D}^1(\mathcal{R})$ as the only variable, governed by:

$$\begin{cases} -\operatorname{div}(D \mathbf{grad} \phi) + \Sigma_a \phi = S_f & \text{in } \mathcal{R}, \\ D \partial_n \phi = 0 & \text{on } \Gamma_N, \\ D \partial_n \phi + \alpha \phi = 0 & \text{on } \Gamma_R. \end{cases} \quad (7)$$

Then, we recover \mathbf{p} using the relation $\mathbf{p} = -D \mathbf{grad} \phi$. About Eqs. (6) and (7), one has the elementary results below (see for instance [9]).

Theorem 1. *There exists a unique solution $\phi \in H_{0,\Gamma_D}^1(\mathcal{R})$ to equations (7).*

2.4. The mixed neutron diffusion equations

Define $\mathbf{H}_{0,\Gamma_N}(\operatorname{div}, \mathcal{R}) := \{\mathbf{q} \in \mathbf{H}(\operatorname{div}, \mathcal{R}) \mid \mathbf{q} \cdot \mathbf{n}|_{\Gamma_N} = 0\}$. By construction, we have that $\mathbf{p} \in \mathbf{H}_{0,\Gamma_N}(\operatorname{div}, \mathcal{R})$ and also $\mathbf{p} \cdot \mathbf{n}|_{\Gamma_R} \in L^2(\Gamma_R)$. So, we introduce the natural functional space and related norm for the currents

$$\mathbf{Q} := \{\mathbf{q} \in \mathbf{H}_{0,\Gamma_N}(\operatorname{div}, \mathcal{R}) \mid \mathbf{q} \cdot \mathbf{n}|_{\Gamma_R} \in L^2(\Gamma_R)\}, \quad \|\mathbf{q}\|_{\mathbf{Q}} := \left(\|\mathbf{q}\|_{\mathbf{H}(\operatorname{div}, \mathcal{R})}^2 + \int_{\Gamma_R} (\mathbf{q} \cdot \mathbf{n})^2 \right)^{1/2}.$$

Since (6) is equivalent to (7), we infer from Theorem 1 the second result below.

Theorem 2. *There exists a unique $(\mathbf{p}, \phi) \in \mathbf{Q} \times H_{0,\Gamma_D}^1(\mathcal{R})$ to equations (6), such that ϕ satisfies (7).*

3. Discretization of the mixed neutron diffusion equations

3.1. The mixed variational formulation

In order to obtain a mixed variational formulation, we multiply the first equation of (6) by a test function $\mathbf{q} \in \mathbf{Q}$, and the second equation by a test function $\psi \in L^2(\mathcal{R})$, and we integrate the two equations on \mathcal{R} to reach:

$$\int_{\mathcal{R}} \left(-\frac{1}{D} \mathbf{p} \cdot \mathbf{q} - \mathbf{grad} \phi \cdot \mathbf{q} + \psi \operatorname{div} \mathbf{p} + \Sigma_a \phi \psi \right) = \int_{\mathcal{R}} S_f \psi.$$

One integrates by parts to remove the first order derivatives of ϕ , so that the only regularity requirement on the flux will be $\phi \in L^2(\mathcal{R})$. Using Green first identity, we have:

$$\int_{\mathcal{R}} (\mathbf{grad} \phi' \cdot \mathbf{q} + \phi' \operatorname{div} \mathbf{q}) = \langle \phi', \mathbf{q} \cdot \mathbf{n} \rangle, \forall (\mathbf{q}, \phi') \in \mathbf{H}(\operatorname{div}, \mathcal{R}) \times H^1(\mathcal{R}) \quad (8)$$

where $\langle \cdot, \cdot \rangle$ denotes the duality pairing on $H' \times H$, with $H = H^{1/2}(\partial\mathcal{R})$. In our case, we have at hand some additional regularity on the boundary, which allows one to replace the duality product $\langle \phi', \mathbf{q} \cdot \mathbf{n} \rangle$ by some integral. Proceeding similarly to [4, 5], one obtains the density result hereafter. The functional space

$$\mathbf{Q}^\infty = \{\mathbf{q} \in C^\infty(\mathcal{R})^d \mid \operatorname{supp}(\mathbf{q}) \text{ is compact in } \mathcal{R} \cup \Gamma_D \cup \Gamma_R\}$$

is dense in \mathbf{Q} . With this result, one can replace $\mathbf{q} \in \mathbf{Q}$ by smooth fields of \mathbf{Q}^∞ and then pass to the limit, to reach

$$\int_{\mathcal{R}} (\mathbf{grad} \phi' \cdot \mathbf{q} + \phi' \operatorname{div} \mathbf{q}) = \int_{\Gamma_R} \phi' (\mathbf{q} \cdot \mathbf{n}), \forall (\mathbf{q}, \phi') \in \mathbf{Q} \times H_{0,\Gamma_D}^1(\mathcal{R}). \quad (9)$$

Using finally the boundary condition on Γ_R in (6), one reaches a mixed variational formulation governing (\mathbf{p}, ϕ) :

Find $(\mathbf{p}, \phi) \in \mathbf{Q} \times L^2(\mathcal{R})$ such that $\forall (\mathbf{q}, \psi) \in \mathbf{Q} \times L^2(\mathcal{R})$:

$$\int_{\mathcal{R}} \left(-\frac{1}{D} \mathbf{p} \cdot \mathbf{q} + \phi \operatorname{div} \mathbf{q} + \psi \operatorname{div} \mathbf{p} + \Sigma_a \phi \psi \right) - \int_{\Gamma_R} \frac{1}{\alpha} (\mathbf{p} \cdot \mathbf{n})(\mathbf{q} \cdot \mathbf{n}) = \int_{\mathcal{R}} S_f \psi. \quad (10)$$

Theorem 3. *Assume that $0 < (\Sigma_a)_* \leq \Sigma_a \leq (\Sigma_a)^*$ almost everywhere. Then, there exists a unique solution $(\mathbf{p}, \phi) \in \mathbf{Q} \times L^2(\mathcal{R})$ of the mixed variational formulation (10), and moreover this solution satisfies (6).*

In D. Schneider's PhD thesis [35], the proof of Thm. 3 is carried out in a classical way [6], in the case of Dirichlet boundary conditions on the whole boundary (ie. $\Gamma_R = \emptyset$). In Appendix A, we propose another proof, based on an alternative formulation that can be found for instance in [12], which applies to the more general case of mixed Dirichlet and Robin boundary conditions. Moreover, this proof allows us to derive easily error estimates for a piecewise continuous neutron flux, which occurs if the coefficient D is itself piecewise constant (heterogeneous case, cf. Subsection 6.2).

We assume from now on that $0 < (\Sigma_a)_* \leq \Sigma_a \leq (\Sigma_a)^*$ almost everywhere.

3.2. Discretization

We study the 3D case. The reactor is modeled by a rectangular cuboid \mathcal{R} , which is discretized by cartesian meshes $(\mathcal{R}_h)_h$, h denoting the mesh size, which goes to zero. A cartesian mesh is made of N distinct rectangular cuboids, such that $\overline{\mathcal{R}}_h = \cup_{n=1}^N \overline{R}_n$. We set: $\overline{R}_n \cap \overline{R}_m = \Gamma_{nm}$ when R_n and R_m are neighbours. As we already mentioned, the cross sections can be highly heterogeneous, see Subsection 6.2. To simplify the presentation, we assume that the cross sections D and Σ_a are piecewise constant, and that the meshes are such that in every cuboid R_n the cross sections are constant.

The discretized space of the current (resp. flux) is embedded in $\mathbf{H}(\text{div}, \mathcal{R})$ (resp. $L^2(\mathcal{R})$). Let's detail the choices of these spaces.

Let $P(R_n)$ be the set of polynomials of R_n . We consider $Q_{l,m,p}(R_n)$ the following subspace of $P(R_n)$:

$$Q_{l,m,p}(R_n) = \left\{ q(x, y, z) \in P(R_n) \mid q(x, y, z) = \sum_{i,j,k=0}^{l,m,p} a_{i,j,k} x^i y^j z^k, a_{i,j,k} \in \mathbb{R} \right\}.$$

We introduce as well the 3D polynomial space $\mathbf{D}_k(R_n)$:

$$\mathbf{D}_k(R_n) = [Q_{k,k-1,k-1}(R_n) \times \mathbf{0} \times \mathbf{0}] \oplus [\mathbf{0} \times Q_{k-1,k,k-1}(R_n) \times \mathbf{0}] \oplus [\mathbf{0} \times \mathbf{0} \times Q_{k-1,k-1,k}(R_n)].$$

We are now in a position to define the so-called Raviart-Thomas-Nédélec (or RTN) finite element, cf. [33, 29]: consider $\mathbf{Q}_h^k \subset \mathbf{H}(\text{div}, \mathcal{R})$ (resp. $V_h^k \subset L^2(\mathcal{R})$) the discretized spaces (recall that h is the mesh size). We set:

$$\begin{aligned} \mathbf{Q}_h^k &= \{ \mathbf{q} \in \mathbf{H}(\text{div}, \mathcal{R}_h) \mid \forall n \in \{1, \dots, N\}, \mathbf{q}|_{R_n} \in \mathbf{D}_k(R_n) \}, \\ V_h^k &= \{ \psi \in L^2(\mathcal{R}_h) \mid \forall n \in \{1, \dots, N\}, \psi|_{R_n} \in Q_{k-1,k-1,k-1}(R_n) \}. \end{aligned} \tag{11}$$

Remark 1. Note that the Neumann boundary condition corresponds to essential boundary conditions for the discrete vector fields, so that we will have to eliminate the degrees of freedom on Γ_N if it exists. By construction, for all $\mathbf{q} \in \mathbf{Q}_h^k$, one has automatically that $\mathbf{q} \cdot \mathbf{n}|_{\partial\mathcal{R}} \in L^2(\partial\mathcal{R})$, and it follows that $\mathbf{Q}_h^k \subset \mathbf{Q}$. In other words, the discretization $\mathbf{Q}_h^k \times V_h^k$ is conforming in $\mathbf{Q} \times L^2(\mathcal{R})$. Moreover, we have $\text{div } \mathbf{Q}_h^k \subset V_h^k$: consistency is ensured.

The discrete variational formulation reads:

Find $(\mathbf{p}_h, \phi_h) \in \mathbf{Q}_h^k \times V_h^k$ such that $\forall (\mathbf{q}_h, \psi_h) \in \mathbf{Q}_h^k \times V_h^k$:

$$\int_{\mathcal{R}} \left(-\frac{1}{D} \mathbf{p}_h \cdot \mathbf{q}_h + \phi_h \text{div } \mathbf{q}_h + \psi_h \text{div } \mathbf{p}_h + \Sigma_a \phi_h \psi_h \right)$$

$$- \int_{\Gamma_R} \frac{1}{\alpha} (\mathbf{p}_h \cdot \mathbf{n}) (\mathbf{q}_h \cdot \mathbf{n}) = \int_{\mathcal{R}} S_{f,h} \psi_h. \quad (12)$$

Theorem 4. *The discrete solution converges to the exact solution as h goes to zero. Moreover, if $\phi \in H^f(\mathcal{R})$, $\mathbf{p} \in H^p(\mathcal{R})^d$ and $\operatorname{div} \mathbf{p} \in H^{p'}(\mathcal{R})$ with $f, p, p' \geq 1$, there holds*

$$\|\mathbf{p} - \mathbf{p}_h\|_{\mathbf{H}(\operatorname{div}, \mathcal{R})} + \|\phi - \phi_h\|_0 \leq C h^{\min(k, f, p, p')} (|\phi|_f + |\mathbf{p}|_p + |\operatorname{div} \mathbf{p}|_{p'}), \quad (13)$$

with $C > 0$ independent of h .

To our knowledge this error estimate is new compared to the classical one given in [10]. We prove Thm. 4 in Appendix B.

Several illuminating comments can be made about these convergence results:

- One has always $\phi \in H^1(\mathcal{R})$.
- On the other hand, if S_f belongs to $L^2(\mathcal{R})$ (minimal regularity), then $\operatorname{div} \mathbf{p} = S_f - \Sigma_a \phi \in L^2(\mathcal{R})$ according to (7).
- Suppose that $D = 1$ over \mathcal{R} : as a consequence, the relation between ϕ and \mathbf{p} reads $\mathbf{p} = -\mathbf{grad} \phi$. It follows that the regularity of the vector field \mathbf{p} is always equal to that of the scalar field ϕ minus one: $p = f - 1$.
- Suppose still that $D = 1$ over \mathcal{R} : then $\mathbf{p} \in L^2(\mathcal{R})^d$, $\mathbf{rot} \mathbf{p} = 0$ and $\operatorname{div} \mathbf{p} \in L^2(\mathcal{R})$. In addition, the boundary conditions yield $\mathbf{p} \times \mathbf{n}_{\Gamma_D} = 0$ (because $\phi|_{\Gamma_D} = 0$), $\mathbf{p} \cdot \mathbf{n}_{\Gamma_N} = 0$, and $\mathbf{p} \cdot \mathbf{n}_{\Gamma_R} \in H^{1/2}(\Gamma_R)$. According to [15, 16], one has $\mathbf{p} \in H^p(\mathcal{R})^d$, with $p > 1/4$ in all configurations, and $p > 1/2$ provided that Γ_D is perpendicular to Γ_N and Γ_R .
- The estimate (13) can be generalized in the following way. Following the proofs given in [34], one finds that the regularity assumptions on ϕ , \mathbf{p} and $\operatorname{div} \mathbf{p}$ need only to be local. In other words, only *piecewise regularity* of the solution is required for (13) to hold, which can be of great importance if the coefficients D and Σ_a are themselves piecewise constant coefficients.

3.3. The linear system

Let's split \mathbf{Q}_h^k and V_h^k into the following basis:

$$\begin{aligned} \mathbf{Q}_h^k &= \operatorname{vect} \left((q_{x,i} \mathbf{x})_{1 \leq i \leq N_x}, (q_{y,j} \mathbf{y})_{1 \leq j \leq N_y}, (q_{z,k} \mathbf{z})_{1 \leq k \leq N_z} \right), \\ V_h^k &= \operatorname{vect} \left((\psi_l)_{1 \leq l \leq N_\phi} \right), \end{aligned}$$

so that: $\mathbf{p}_h = \sum_{d=x,y,z} \sum_{i=1}^{N_d} p_{d,i} q_{d,i} \mathbf{d}$, and $\phi_h = \sum_{l=1}^{N_\phi} \phi_l \psi_l$. We set $\underline{\mathbf{p}} = (\underline{\mathbf{p}}_x, \underline{\mathbf{p}}_y, \underline{\mathbf{p}}_z)^T$,

with (for $d = x, y, z$): $\underline{\mathbf{p}}_d = (p_{d,1}, \dots, p_{d,N_d})^T$, and $\underline{\phi} = (\phi_1, \dots, \phi_{N_\phi})^T$.

Suppose (for simplicity) that $\Gamma_D = \partial\mathcal{R}$. The linear system, our *discrete source solver*, corresponding to the variational formulation (12) reads:

$$\begin{pmatrix} -\mathbb{A} & \mathbb{B} \\ \mathbb{B}^T & \mathbb{T} \end{pmatrix} \begin{pmatrix} \underline{\mathbf{p}} \\ \underline{\phi} \end{pmatrix} = \begin{pmatrix} 0 \\ \underline{\mathbf{S}}_f \end{pmatrix}, \quad (14)$$

with the following matrices:

- $\mathbb{A} \in \mathbb{R}^{N \times N}$, $N = \sum_{d=x,y,z} N_d$ is a block-diagonal matrix with diagonal blocks

$\mathbb{A}_d \in \mathbb{R}^{N_d \times N_d}$. $d = x, y, z$ such that: $(\mathbb{A}_d)_{i,j} = \int_{\mathcal{R}_h} \frac{1}{D_h} q_{i,d} q_{j,d}$. The current mass matrices $(\mathbb{A}_d)_d$ are symmetric positive definite matrices.

- $\mathbb{B} = (\mathbb{B}_x, \mathbb{B}_y, \mathbb{B}_z)^T \in \mathbb{R}^{N \times N_\phi}$, such that $\mathbb{B}_d \in \mathbb{R}^{N_d \times N_\phi}$ $(\mathbb{B}_d)_{i,j} = \int_{\mathcal{R}_h} \partial_d q_{d,i} \psi_j$,

- $\mathbb{T} \in \mathbb{R}^{N_\phi \times N_\phi}$, such that: $\mathbb{T}_{i,j} = \int_{\mathcal{R}_h} \Sigma_{a,h} \psi_i \psi_j$. The flux mass matrix \mathbb{T} is a symmetric positive definite matrix.

- $\underline{\mathbf{S}}_f \in \mathbb{R}^{N_\phi}$ such that: $(\underline{\mathbf{S}}_f)_i = \int_{\mathcal{R}_h} S_{f,h} \psi_i$.

When using RTN finite elements, \mathbb{T} is diagonal, the $(\mathbb{A}_d)_d$ are block-diagonal matrices (there are only local couplings), and the coupling matrices $(\mathbb{B}_d)_d$ are very simple, containing 1 or -1 terms. The linear system (14) can be read this way:

$$\begin{cases} \mathbb{W}_d \underline{\mathbf{p}}_d + \sum_{d' \neq d} \mathbb{B}_d \mathbb{T}^{-1} \mathbb{B}_{d'}^T \underline{\mathbf{p}}_{d'} = \mathbb{B}_d \mathbb{T}^{-1} \underline{\mathbf{S}}_f, \\ \mathbb{T} \underline{\phi} = \underline{\mathbf{S}}_f - \sum_d \mathbb{B}'_d \underline{\mathbf{p}}_{d'}, \end{cases} \quad (15)$$

with $\mathbb{W}_d = \mathbb{A}_d + \mathbb{B}_d \mathbb{T}^{-1} \mathbb{B}_d^T$. $(\mathbb{W}_d)_d$ are symmetric positive definite matrices, with the same structure than the one of $(\mathbb{A}_d)_d$.

In the MINOS solver, our (discrete) source solver is implemented by means of a block Gauss-Seidel method (it corresponds to an alternating direction algorithm). In practice, the inverse power iteration leads convergence, so that a single inner iteration is actually required. This interesting property

will be used throughout the paper to simplify the algorithms and their implementation. A Cholesky algorithm is applied to solve each diagonal block $\mathbb{W}_d \underline{\mathbf{p}}_d = RHS$. Finally, the matrices $\mathbb{B}_d \mathbb{T}^{-1} \mathbb{B}_d^T$ are not build explicitly, to save memory (the drawback being that we cannot use an external solver).

4. Domain decomposition with the Schwarz iterative algorithm

4.1. Presentation

Schwarz iterative algorithm was designed in 1869 [36] in order to study the Laplace operator on irregular domains: Hermann Schwarz's original idea was to split the original domain into *overlapping* regular subdomains (such as rectangles or disks) and to write an iterative solver using solutions on the regular subdomains to converge to the global solution on the irregular domain. In our case, we choose a *nonoverlapping* splitting into N_{DD} subdomains, namely $\overline{\mathcal{R}} = \sum_{I=1, \dots, N_{DD}} \overline{\mathcal{R}}_I$, with $\mathcal{R}_I \cap \mathcal{R}_{I'} = \emptyset$ for $I \neq I'$. The non-empty interfaces are denoted by $\Gamma_{IJ} = \text{int}(\overline{\mathcal{R}}_I \cap \overline{\mathcal{R}}_J)$. For $I = 1, \dots, N_{DD}$, we let \mathbf{n}_I be the outward unit normal vector to $\partial \mathcal{R}_I$ and we set $\Gamma_I = \text{int}(\partial \mathcal{R} \cap \partial \mathcal{R}_I)$. Without loss of generality, in this rest of the paper, we consider the case of two subdomains, that is $N_{DD} = 2$. We then use the following notations: interface $\Gamma = \text{int}(\overline{\mathcal{R}}_1 \cap \overline{\mathcal{R}}_2)$ (note that $\mathbf{n}_1 = -\mathbf{n}_2$ on Γ), whereas the index I spans $\{1, 2\}$, and the associated indices J are such that (I, J) spans $\{(1, 2), (2, 1)\}$ (which corresponds to the oriented interface Γ , equal to Γ_{12} or Γ_{21}).

4.2. The Schwarz iterative algorithm

Let's detail this algorithm for the mixed neutrons diffusion equations, where we assume for simplicity zero flux boundary condition on $\partial \mathcal{R}$: namely, $\Gamma_N = \Gamma_R = \emptyset$. We consider equations (6). Let us set $(\mathbf{p}_I, \phi_I) = (\mathbf{p}, \phi)|_{\mathcal{R}_I}$, where (\mathbf{p}, ϕ) is the unique solution to (6). Then, $(\mathbf{p}_I, \phi_I)_I$ are governed by: Find $(\mathbf{p}_I, \phi_I) \in \mathbf{H}(\text{div}, \mathcal{R}_I) \times H_{0, \Gamma_I}^1(\mathcal{R}_I)$, such that:

$$\left\{ \begin{array}{ll} \frac{1}{D} \mathbf{p}_I + \mathbf{grad} \phi_I = 0, & \text{in } \mathcal{R}_I, \\ \text{div} \mathbf{p}_I + \Sigma_a \phi_I = S_{f, I}, & \text{in } \mathcal{R}_I, \\ \phi_1 = \phi_2, & \text{on } \Gamma, \\ -\mathbf{p}_1 \cdot \mathbf{n}_1 = \mathbf{p}_2 \cdot \mathbf{n}_2, & \text{on } \Gamma. \end{array} \right. \quad (16)$$

On the other hand, if $(\mathbf{p}_I, \phi_I)_I$ solve (16), then

$$(\mathbf{p}, \phi) = \begin{cases} (\mathbf{p}_1, \phi_1) & \text{in } \mathcal{R}_1 \\ (\mathbf{p}_2, \phi_2) & \text{in } \mathcal{R}_2 \end{cases} \quad (17)$$

obviously solves (6). We provide in Appendix C an alternate proof of this result, based on energy estimates.

We remark that the interface conditions in (16), namely $\phi_1 = \phi_2$ and $-\mathbf{p}_1 \cdot \mathbf{n}_1 = \mathbf{p}_2 \cdot \mathbf{n}_2$ on Γ , can be equivalently replaced by the following Robin interface conditions:

$$\begin{cases} -\mathbf{p}_1 \cdot \mathbf{n}_1 + \alpha_1 \phi_1 = \mathbf{p}_2 \cdot \mathbf{n}_2 + \alpha_1 \phi_2 & \text{on } \Gamma, \\ -\mathbf{p}_2 \cdot \mathbf{n}_2 + \alpha_2 \phi_2 = \mathbf{p}_1 \cdot \mathbf{n}_1 + \alpha_2 \phi_1 & \text{on } \Gamma, \end{cases} \quad (18)$$

with $\alpha_1, \alpha_2 > 0$. Indeed, the difference of these two conditions returns the Dirichlet interface condition, and one recovers then the Neumann interface condition.

We want to compute (\mathbf{p}_1, ϕ_1) and (\mathbf{p}_2, ϕ_2) separately. As we do not know the value of the unknowns on Γ , we can either use a Lagrange multiplier to dualize the interface conditions on Γ [23]; or solve this problem iteratively, using some interface conditions to exchange informations. In the latter case, if one uses only the Dirichlet or the Neumann interface condition as in (16), one needs an overlap between the subdomains to recover information [24]. On the other hand, Robin interface conditions allow convergence without overlap [25, 31]. Thus, we shall use the following Schwarz iterative algorithm [17]:

Setting $(\mathbf{p}_I^0, \phi_I^0) \in \mathbf{H}(\text{div}, \mathcal{R}_I) \times H_{0,\Gamma}^1(\mathcal{R}_I)$,

Find $(\mathbf{p}_I^{n+1}, \phi_I^{n+1}) \in \mathbf{H}(\text{div}, \mathcal{R}_I) \times H_{0,\Gamma}^1(\mathcal{R}_I)$, $\forall n \in \mathbb{N}$, such that:

$$\begin{cases} \frac{1}{D} \mathbf{p}_I^{n+1} + \mathbf{grad} \phi_I^{n+1} = 0, & \text{in } \mathcal{R}_I, \\ \text{div} \mathbf{p}_I^{n+1} + \Sigma_a \phi_I^{n+1} = S_{f,I}, & \text{in } \mathcal{R}_I, \\ -\mathbf{p}_1^{n+1} \cdot \mathbf{n}_1 + \alpha_1 \phi_1^{n+1} = \mathbf{p}_2^n \cdot \mathbf{n}_2 + \alpha_1 \phi_2^n, & \text{on } \Gamma, \\ -\mathbf{p}_2^{n+1} \cdot \mathbf{n}_2 + \alpha_2 \phi_2^{n+1} = \mathbf{p}_1^{n(+1)} \cdot \mathbf{n}_1 + \alpha_2 \phi_1^{n(+1)}, & \text{on } \Gamma. \end{cases} \quad (19)$$

From a computational point of view, this method is rather easy to implement, provided one has subdomain solvers for the problems

Find $(\mathbf{p}'_I, \phi'_I) \in \mathbf{H}(\text{div}, \mathcal{R}_I) \times H^1_{0,\Gamma_I}(\mathcal{R}_I)$, such that:

$$\begin{cases} \frac{1}{D}\mathbf{p}'_I + \mathbf{grad} \phi'_I = 0, & \text{in } \mathcal{R}_I, \\ \text{div } \mathbf{p}'_I + \Sigma_a \phi'_I = S', & \text{in } \mathcal{R}_I, \\ -\mathbf{p}'_I \cdot \mathbf{n}_I + \alpha_I \phi'_I = s', & \text{on } \Gamma, \end{cases}$$

at hand. We just have to ensure the data transfer between the subdomains given by the interface conditions. Note that setting at each iteration step n : $-\mathbf{p}_2^{n+1} \cdot \mathbf{n}_2 + \alpha_2 \phi_2^{n+1} = \mathbf{p}_1^n \cdot \mathbf{n}_1 + \alpha_2 \phi_1^n$, the Schwarz iterative algorithm is parallel: we can solve the problems on \mathcal{R}_1 and \mathcal{R}_2 simultaneously. This algorithm is known as the additive Schwarz method (ASM). We will see that after discretization, from an algebraic point of view, it corresponds to a block Jacobi algorithm. On the contrary, setting at each iteration n : $-\mathbf{p}_2^{n+1} \cdot \mathbf{n}_2 + \alpha_2 \phi_2^{n+1} = \mathbf{p}_1^{n+1} \cdot \mathbf{n}_1 + \alpha_2 \phi_1^{n+1}$, the Schwarz iterative algorithm is sequential: we must solve first the problem on \mathcal{R}_1 , then the problem on \mathcal{R}_2 . This algorithm is known as the multiplicative Schwarz method (MSM). After discretization, it corresponds to a block Gauss-Seidel algorithm. Let us see how this algorithm modifies the eigenvalue algorithm described in Section 2.1.

4.3. The inverse power algorithm with domain decomposition

Applying Schwarz iterative method to algorithm (5), at iteration number $m + 1$, we should compute the solution to the source solver iteratively, which yields in principle nested outer ($m \leftarrow m + 1$) and inner (index n) iterations. However, as we already mentioned, numerical experiments show that the inverse power algorithm leads the global convergence: a single inner iteration is sufficient. Hence, the resulting algorithm contains only one level of iteration (with index m). The inverse power algorithm with domain decomposition reads then:

Set $(\mathbf{p}_I^0, \phi_I^0)_I, k_{eff}^0, m = 0$.

Until convergence, do: $m \leftarrow m + 1$

Solve:

$$\begin{cases} \frac{1}{D} \mathbf{p}_I^{m+1} + \mathbf{grad} \phi_I^{m+1} = 0, & \text{in } \mathcal{R}_I, \\ \operatorname{div} \mathbf{p}_I^{m+1} + \Sigma_a \phi_I^{m+1} = \frac{1}{k_{eff}^m} \Sigma_f \phi_I^m, & \text{in } \mathcal{R}_I, \\ -\mathbf{p}_I^{m+1} \cdot \mathbf{n}_I + \alpha_I \phi_I^{m+1} = \mathbf{p}_J^{m(+1)} \cdot \mathbf{n}_J + \alpha_I \phi_J^{m(+1)}, & \text{on } \Gamma, \\ \phi_I^{m+1} = 0, & \text{on } \partial\mathcal{R} \cap \partial\mathcal{R}_I, \end{cases} \quad (20)$$

$$\text{Compute } k_{eff}^{m+1} = k_{eff}^m \frac{\sum_{I=1}^2 \int_{\mathcal{R}_I} (\Sigma_f \phi_I^{m+1})^2}{\sum_{I=1}^2 \int_{\mathcal{R}_I} (\Sigma_f \phi_I^{m+1} \Sigma_f \phi_I^m)}.$$

End

Compared with algorithm (5), we handle a Robin interface condition.

4.4. Convergence

We show the convergence of (19) with³ $\alpha_1 = \alpha_2 = \alpha > 0$.

Proposition 5. *Assume that the solution to (6) is such that $\mathbf{p} \cdot \mathbf{n}|_\Gamma \in L^2(\Gamma)$. Choose $(\mathbf{p}^0, \phi^0) \in \mathbf{Q} \times H_0^1(\mathcal{R})$, with $\mathbf{p}^0 \cdot \mathbf{n}|_\Gamma \in L^2(\Gamma)$.*

We set $(\mathbf{p}_2^0, \phi_2^0) = (\mathbf{p}^0, \phi^0)|_{\mathcal{R}_2}$ for the MSM, and $(\mathbf{p}_I^0, \phi_I^0) = (\mathbf{p}^0, \phi^0)|_{\mathcal{R}_I}$ for the ASM. We consider the sequences $(\mathbf{p}_I^n, \phi_I^n)_{n \in \mathbb{N}}$ in $\mathbf{H}(\operatorname{div}, \mathcal{R}_I) \times H^1(\mathcal{R}_I)$ satisfying (19). Then the sequences $(\mathbf{p}_I^n, \phi_I^n)_{n \in \mathbb{N}}$ tend to (\mathbf{p}_I, ϕ_I) satisfying (16), in $\mathbf{H}(\operatorname{div}, \mathcal{R}_I) \times H^1(\mathcal{R}_I)$.

Remark 2. *The assumption on \mathbf{p} is not very restrictive. Indeed, in the same spirit as the comments of Subsection 3.2, consider the case $D = 1$ over \mathcal{R} . Then, $\mathbf{p} = -\mathbf{grad} \phi$, with $\phi \in H_0^1(\mathcal{R})$ and $\Delta \phi \in L^2(\mathcal{R})$. As we know from [15, 16], one has $\phi \in H^f(\mathcal{R})$ for some $f > 3/2$, so $\mathbf{p} \in H^p(\mathcal{R})^d$ for $p = f - 1 > 1/2$, and in particular $\mathbf{p} \cdot \mathbf{n}|_\Gamma \in L^2(\Gamma)$. In the more general cases ($\Gamma_N \neq \emptyset$ and/or $\Gamma_R \neq \emptyset$), one recovers a similar result. For that, it is enough to choose an interface Γ whose boundary $\partial\Gamma$ does not meet $\bar{\Gamma}_D \cap \bar{\Gamma}_N$, $\bar{\Gamma}_N \cap \bar{\Gamma}_R$, or $\bar{\Gamma}_R \cap \bar{\Gamma}_D$, that is where the change of boundary condition occurs.*

The proof of Prop. 5 is given in Appendix D.

³To our knowledge, there is no available proof in the case where $\alpha_1 \neq \alpha_2$.

4.5. Optimizing the α parameter

In order to choose the α parameter, we study the following asymptotic problem, as in [27]: Let $\mathcal{R} = \mathbb{R}^2$ be split between two subdomains $\mathcal{R}_1 =]-\infty, 0[\times \mathbb{R}$ and $\mathcal{R}_2 =]0, +\infty[\times \mathbb{R}$, so that the interface is $\Gamma : \{(x, y) | x = 0\}$. We have $\mathbf{n}_1 = \mathbf{x}$ and $\mathbf{n}_2 = -\mathbf{x}$. Given ϕ^0 , we set $\phi_I^0 = (\phi^0)|_{\mathcal{R}_I}$. In each subdomain \mathcal{R}_I , we suppose that the diffusion coefficient $D_I = D|_{\mathcal{R}_I}$ and the absorption cross section $\Sigma_{a,I} = \Sigma_a|_{\mathcal{R}_I}$ are constant. The Schwarz additive iterative algorithm for the primal neutron diffusion equation, with Robin interface conditions reads:

find $\phi_I^{n+1} \in H^1(\mathcal{R}_I)$, $\forall n \in \mathbb{N}$, such that:

$$\begin{cases} -\Delta \phi_I^{n+1} + \frac{\Sigma_{a,I}}{D_I} \phi_I^{n+1} = \frac{1}{D_I} S_{f,I}, & \text{in } \mathcal{R}_I, \\ D_1 \partial_x \phi_1^{n+1} + \alpha_1 \phi_1^{n+1} = D_2 \partial_x \phi_2^n + \alpha_1 \phi_2^n, & \text{on } \Gamma, \\ -D_2 \partial_x \phi_2^{n+1} + \alpha_2 \phi_2^{n+1} = -D_1 \partial_x \phi_1^n + \alpha_2 \phi_1^n, & \text{on } \Gamma. \end{cases} \quad (21)$$

Let us study the errors with the help of the partial Fourier transform along the y axis, which is defined by, for $f \in \mathcal{L}^1(\mathbb{R})$:

$$\forall (x, k) \in \hat{\mathcal{R}} := \mathbb{R}^2, \quad \hat{f}(x, k) := \int_{\mathbb{R}} \exp(-iky) f(x, y) dy. \quad (22)$$

Suppose that f is smooth enough. After integrating by parts twice, we have:

$$\widehat{\Delta f} = \int_{\mathbb{R}} \exp(-iky) \Delta f(x, y) dy = -\partial_{xx}^2 \hat{f} + k^2 \hat{f}. \quad (23)$$

Let \hat{e}_I^n be the partial Fourier transform in the y direction of e_I^n . The Fourier transform of (21), with unknowns e_I^n (and no source terms) reads:

$\forall n \in \mathbb{N}$:

$$\begin{cases} -\partial_{xx}^2 \hat{e}_I^{n+1} + \left(k^2 + \frac{\Sigma_{a,I}}{D_I} \right) \hat{e}_I^{n+1} = 0, & \text{in } \hat{\mathcal{R}}_I, \\ D_1 \partial_x \hat{e}_1^{n+1} + \alpha_1 \hat{e}_1^{n+1} = D_2 \partial_x \hat{e}_2^n + \alpha_1 \hat{e}_2^n, & \text{on } \Gamma, \\ -D_2 \partial_x \hat{e}_2^{n+1} + \alpha_2 \hat{e}_2^{n+1} = -D_1 \partial_x \hat{e}_1^n + \alpha_2 \hat{e}_1^n, & \text{on } \Gamma. \end{cases} \quad (24)$$

We set: $\lambda_I := \lambda_I(k) = \sqrt{k^2 + \frac{\Sigma_{a,I}}{D_I}}$. According to the first equation of (24), and in order to have vanishing errors at $\pm\infty$, one finds that:

$$\forall n \in \mathbb{N}^*, \quad \hat{e}_1^n(x, k) = B_1^n \exp(\lambda_1 x) \text{ and } \hat{e}_2^n(x, k) = B_2^n \exp(-\lambda_2 x). \quad (25)$$

Above, $B_1^n := B_1^n(k)$ and $B_2^n := B_2^n(k)$ are constant coefficients. Obviously, one looks for coefficients such that $\lim_{n \rightarrow \infty} B_I^n = 0$, with the "fastest" possible convergence rate.

Their values can be derived by writing the interface conditions explicitly. Indeed, for all $n \in \mathbb{N}^*$, one finds $B_I^{n+1}(\alpha_I + D_I \lambda_I) = B_J^n(\alpha_J - D_I \lambda_I)$. By induction, this yields:

$$I = 1, 2, \forall n \in \mathbb{N}^*, B_I^{n+2} = \rho B_I^n, \text{ with } \rho = \frac{(\alpha_1 - D_2 \lambda_2)(\alpha_2 - D_1 \lambda_1)}{(\alpha_1 + D_1 \lambda_1)(\alpha_2 + D_2 \lambda_2)}. \quad (26)$$

As $\alpha_I > 0$, $D_I > 0$ and $\lambda_I > 0$, one has $0 \leq \rho < 1$. The smaller ρ , the better the convergence rate. In the limit cases where both $\alpha_I = 0$ (Neumann interface condition only) or both $\alpha_I \rightarrow +\infty$ (Dirichlet interface condition only), one finds $\rho = 1$: the coefficients $(B_I^n)_n$ do not go to zero, ie. the non-overlapping Schwarz method does not converge.

As ϕ^0 is not the exact solution, the errors of the first step e_1^1 and e_2^1 are not zeros, so that $B_I^1 \neq 0$, cf. (25). On the other hand, one has $B_I^{n+2} = \rho B_I^n$ for $n > 0$, cf. (26). So, if $\rho = 0$, convergence is achieved at the second step. In the more general case of N subdomains built as strips, one can check that convergence can not be achieved in less than N steps [27].

In order to reduce ρ , we need to have $\alpha_I \approx D_J \lambda_J$. At the order 0 in k , it means that the optimal parameters are governed by the relation:

$$\alpha_I = \sqrt{\Sigma_{a,J} D_J}. \quad (27)$$

A better choice is to take α_I as a function of k^2 . Taking the inverse Fourier transform, this corresponds to have second order derivatives along the y axis in the interface conditions (ie. second order tangential derivatives). This kind of interface conditions are known as Ventcell interface conditions. They can be used when the solution is smooth enough, and their use improves the convergence rate [20].

Note that the condition (27) targets the damping of slow variations along the interface. In order to damp (roughly) all frequencies, one can choose $\alpha_I = \alpha_{opt}$ defined as in [13, 20]:

$$\alpha_{opt} = \min_{\alpha_1, \alpha_2} \max_k \frac{(\alpha_1 - D_2 \lambda_2(k)) (\alpha_2 - D_1 \lambda_1(k))}{(\alpha_1 + D_1 \lambda_1(k)) (\alpha_2 + D_2 \lambda_2(k))}. \quad (28)$$

Suppose that $\Sigma_{a,1} = \Sigma_{a,2}$ and $D_1 = D_2$, so that we can set $\alpha = \alpha_1 = \alpha_2$. Notice that numerically we have $|k| \leq \pi/h$, where h is the mesh step. Hence,

one can restrict the set of relevant values of α to the following interval:

$$\left[\sqrt{\Sigma_a D}, \sqrt{\Sigma_a D + D^2 \frac{\pi^2}{h^2}} \right]. \quad (29)$$

This approach is extensively studied in [13]. At order 0 in k , the solution is then the geometrical mean between the maximal and the minimal values of α , namely:

$$\alpha = \left(\sqrt{\Sigma_a D} \sqrt{\Sigma_a D + D^2 \frac{\pi^2}{h^2}} \right)^{1/2} \quad (30)$$

Remark 3. *In our numerical experiments, the neutrons flux is quite smooth: we can stick to the Robin boundary conditions (18), with $\alpha_I = \sqrt{\Sigma_a|_{\mathcal{R}_I} D|_{\mathcal{R}_I}}$, so that one can have $\alpha_1 \neq \alpha_2$. Also, if $\Sigma_a|_{\mathcal{R}_I}$ and/or $D|_{\mathcal{R}_I}$ change from one cuboid to the other, so does the value of α_J at the corresponding part of the interface. When solving the multigroup diffusion equations, we have different α^g -parameters for each group, since the macroscopic cross sections and the diffusion coefficient change from one group to another. We have for each group $\alpha_I^g = \sqrt{\Sigma_a^g|_{\mathcal{R}_I} D^g|_{\mathcal{R}_I}}$.*

5. The discretization of the Schwarz iterative algorithm

5.1. The variational formulation

In order to write the $\mathbf{H}(\text{div}, \mathcal{R}_I) \times L^2(\mathcal{R}_I)$ -conforming variational formulation of equations (19), we introduce

$$\mathbf{Q}_I^+ := \{\mathbf{q} \in \mathbf{H}(\text{div}, \mathcal{R}_I) \mid \mathbf{q} \cdot \mathbf{n}_\Gamma \in L^2(\Gamma)\}$$

together with the following bilinear and continuous forms:

- the symmetric and positive definite forms $a_I : \mathbf{Q}_I^+ \times \mathbf{Q}_I^+ \rightarrow \mathbb{R}$, defined by:

$$a_I(\mathbf{p}_I, \mathbf{q}_I) = \int_{\mathcal{R}_I} \frac{1}{D} \mathbf{p}_I \cdot \mathbf{q}_I + \int_\Gamma \frac{1}{\alpha_J} (\mathbf{p}_I \cdot \mathbf{n}_I) (\mathbf{q}_I \cdot \mathbf{n}_I);$$

- the symmetric and positive definite forms $t_I : L^2(\mathcal{R}_I) \times L^2(\mathcal{R}_I) \rightarrow \mathbb{R}$, defined by:

$$t_I(\phi_I, \psi_I) = \int_{\mathcal{R}_I} \Sigma_a \phi_I \psi_I;$$

• the forms $b_I : \mathbf{Q}_I^+ \times L^2(\mathcal{R}_I) \rightarrow \mathbb{R}$, defined by:

$$b_I(\mathbf{q}_I, \psi_I) = \int_{\mathcal{R}_I} \psi_I \operatorname{div} \mathbf{q}_I.$$

We choose $(\mathbf{p}_I^0, \phi_I^0) \in \mathbf{Q}_I^+ \times L^2(\mathcal{R}_I)$. Using the interface conditions on Γ , integrating by parts and bearing in mind that $\mathbf{n}_2 = -\mathbf{n}_1$ there, we write the variational formulation of equations (19) as follows:

Find $(\mathbf{p}_I^n, \phi_I^n) \in \mathbf{Q}_I^+ \times L^2(\mathcal{R}_I)$, $\forall n \in \mathbb{N}^*$ such that $\forall (\mathbf{q}_I, \psi_I) \in \mathbf{Q}_I^+ \times L^2(\mathcal{R}_I)$:

$$\begin{aligned} & -a_I(\mathbf{p}_I^{n+1}, \mathbf{q}_I) + b_I(\mathbf{q}_I, \phi_I^{n+1}) + b_I(\mathbf{p}_I^{n+1}, \psi_I) + t(\phi_I^{n+1}, \psi_I) \\ & = \langle \phi_J^n, \mathbf{q}_I \cdot \mathbf{n}_I \rangle - \int_{\Gamma} \frac{1}{\alpha_I} (\mathbf{p}_J^n \cdot \mathbf{n}_I) (\mathbf{q}_I \cdot \mathbf{n}_I) + \int_{\mathcal{R}_I} S_f \psi_I. \end{aligned}$$

Remark 4. *This formulation clearly applies to the additive algorithm. It also applies to the multiplicative version, but only for $(I, J) = (1, 2)$, whereas for $(I, J) = (2, 1)$, one has to increment the index n at the right-hand side, so the data is actually $(\phi_J^{n+1}, \mathbf{p}_J^{n+1})$.*

However, this formulation remains formal, because the term $\langle \phi_J^n, \mathbf{q}_I \cdot \mathbf{n}_I \rangle$ is meaningless when one assumes only that ϕ_J^n belongs to $L^2(\mathcal{R}_J)$, as we do in the above variational formulation. If one keeps the interface integral term $\langle \phi_J^n, \mathbf{q}_I \cdot \mathbf{n}_I \rangle$, this leads to an *unstable* numerical scheme. Therefore, we have to write it as a volume integral. Moreover, since this involves the quantity ϕ_J^n defined over the neighbouring subdomain \mathcal{R}_J , the volume integral is over \mathcal{R}_J . So we have to extend $\mathbf{q}_I \cdot \mathbf{n}_I|_{\Gamma}$ there. Mathematically, we recall that $\phi_J^n \in H_{0,\Gamma,J}^1(\mathcal{R}_J)$ in (19), so its trace $\phi_J^n|_{\Gamma}$ belongs to the space of traces on Γ of elements of $H_{0,\Gamma,J}^1(\mathcal{R}_J)$, which we denote by H_{Γ} . One can write

$$\begin{aligned} \langle \phi_J^n, \mathbf{q}_I \cdot \mathbf{n}_I \rangle_{(H_{\Gamma})', H_{\Gamma}} & = \int_{\mathcal{R}_J} \mathbf{grad} \phi_J^n \cdot \tilde{\mathbf{q}}_J + \int_{\mathcal{R}_J} \phi_J^n \operatorname{div} \tilde{\mathbf{q}}_J, \\ & = -a_J(\mathbf{p}_J^n, \tilde{\mathbf{q}}_J) + b_J(\tilde{\mathbf{q}}_J, \phi_J^n). \end{aligned}$$

Above, $\tilde{\mathbf{q}}_J = L_{\nu}(\mathbf{q}_I \cdot \mathbf{n}_I|_{\Gamma})$, where L_{ν} is any continuous lifting operator of the normal trace on Γ , from $(H_{\Gamma})'$ to $\mathbf{H}(\operatorname{div}, \mathcal{R}_J)$. We conclude that the variational formulation of (19) reads (recall that $\mathbf{n}_J = -\mathbf{n}_I$ on Γ):

Find $(\mathbf{p}_I^n, \phi_I^n) \in \mathbf{Q}_I^+ \times L^2(\mathcal{R}_I)$, $\forall n \in \mathbb{N}^*$ such that $\forall (\mathbf{q}_I, \psi_I) \in \mathbf{Q}_I^+ \times L^2(\mathcal{R}_I)$:

$$\begin{aligned} & -a_I(\mathbf{p}_I^{n+1}, \mathbf{q}_I) + b_I(\mathbf{q}_I, \phi_I^{n+1}) + b_I(\mathbf{p}_I^{n+1}, \psi_I) + t(\phi_I^{n+1}, \psi_I) \\ & = - \int_{\Gamma} \frac{1}{\alpha_I} (\mathbf{p}_J^n \cdot \mathbf{n}_I) (\mathbf{q}_I \cdot \mathbf{n}_I) + a_J(\mathbf{p}_J^n, \tilde{\mathbf{q}}_J) - b_J(\tilde{\mathbf{q}}_J, \phi_J^n) + \int_{\mathcal{R}_I} S_f \psi_I. \quad (31) \end{aligned}$$

As noticed above, for the multiplicative version and $(I, J) = (2, 1)$, the data $(\phi_1^n, \mathbf{p}_J^n)$ is replaced by $(\phi_1^{n+1}, \mathbf{p}_J^{n+1})$. From there, discretization follows the guidelines already provided in Subsection 3.2. From a numerical point of view, this allows us to obtain a *stable* numerical scheme.

5.2. Schwarz iterative algorithms from an algebraic point of view

We suppose here, to simplify the notations, that Γ is orthogonal to \mathbf{x} . We will denote by M_i the discretization nodes of the flux, and $P_{d,i}$ the discretization nodes of the d -component of the current.

Let's set $\mathcal{I}_d := \{1, \dots, N_d\}$, $d = x, y, z$, and $\mathcal{I}_\phi := \{1, \dots, N_\phi\}$. We split \mathcal{I}_d and \mathcal{I}_ϕ into the following disjoint subsets:

- $\mathcal{I}_\phi = \mathcal{I}_\phi^1 \cup \mathcal{I}_\phi^2$, such that $\mathcal{I}_\phi^I = \{i \in \mathcal{I}_\phi \mid M_i \in \mathring{\mathcal{R}}_{h,I}\}$,
- For $d = y, z$, $\mathcal{I}_d = \mathcal{I}_d^1 \cup \mathcal{I}_d^2$, such that $\mathcal{I}_d^I = \{i \in \mathcal{I}_d \mid P_{d,i} \in \mathring{\mathcal{R}}_{h,I}\}$,
- $\mathcal{I}_x = \mathcal{I}_x^1 \cup \mathcal{I}_x^2 \cup \mathcal{I}_x^\Gamma$, such that $\mathcal{I}_x^I = \{i \in \mathcal{I}_x \mid P_{x,i} \in \mathring{\mathcal{R}}_{h,I}\}$ and $\mathcal{I}_x^\Gamma := \{i \in \mathcal{I}_x \mid P_{x,i} \in \Gamma\}$.

Below $d = y, z$, with indices I, J as usual.

5.2.1. Back to the linear system (14)

First, we can split the matrices appearing in (14) between these different subsets:

- Splitting of \mathbb{A}_x :

$$\mathbb{A}_x = \begin{pmatrix} \mathring{\mathbb{A}}_x^1 & \left(\mathring{\mathbb{A}}_\Gamma^1\right)^T & 0 \\ \mathring{\mathbb{A}}_\Gamma^1 & \mathbb{A}_\Gamma & \mathring{\mathbb{A}}_x^2 \\ 0 & \left(\mathring{\mathbb{A}}_\Gamma^2\right)^T & \mathring{\mathbb{A}}_x^2 \end{pmatrix} \text{ with } : \begin{cases} \mathring{\mathbb{A}}_x^I & = (\mathbb{A}_x)_{(k,l) \in \mathcal{I}_x^I \times \mathcal{I}_x^I}, \\ \mathbb{A}_\Gamma & = (\mathbb{A}_x)_{(k,l) \in \mathcal{I}_x^\Gamma \times \mathcal{I}_x^\Gamma}, \\ \mathring{\mathbb{A}}_\Gamma^I & = (\mathbb{A}_x)_{(k,l) \in \mathcal{I}_x^\Gamma \times \mathcal{I}_x^I}. \end{cases}$$

\mathbb{A}_Γ is a diagonal matrix such that $\mathbb{A}_\Gamma = \mathbb{A}_\Gamma^1 + \mathbb{A}_\Gamma^2$, with: $(\mathbb{A}_\Gamma^I)_{k,k} = \int_{\mathcal{R}_{h,I}} \frac{1}{D_h} q_{x,k}^2$.

- Splitting of \mathbb{A}_d : $\mathbb{A}_d = \begin{pmatrix} \mathbb{A}_d^1 & 0 \\ 0 & \mathbb{A}_d^2 \end{pmatrix}$ with: $\mathbb{A}_d^I = (\mathbb{A}_d)_{(k,l) \in \mathcal{I}_d^I \times \mathcal{I}_d^I}$.
- Splitting of \mathbb{B}_x : $\mathbb{B}_x = \begin{pmatrix} \mathring{\mathbb{B}}_x^1 & 0 \\ \mathring{\mathbb{B}}_\Gamma^1 & \mathring{\mathbb{B}}_\Gamma^2 \\ 0 & \mathring{\mathbb{B}}_x^2 \end{pmatrix}$ with: $\begin{cases} \mathring{\mathbb{B}}_x^I & = (\mathbb{B}_x)_{(k,l) \in \mathcal{I}_x^I \times \mathcal{I}_\phi^I}, \\ \mathring{\mathbb{B}}_\Gamma^I & = (\mathbb{B}_x)_{(k,l) \in \mathcal{I}_x^\Gamma \times \mathcal{I}_\phi^I}. \end{cases}$

- Splitting of \mathbb{B}_d : $\mathbb{B}_d = \begin{pmatrix} \mathbb{B}_d^1 & 0 \\ 0 & \mathbb{B}_d^2 \end{pmatrix}$ with: $\mathbb{B}_d^I = (\mathbb{B}_d)_{(k,l) \in \mathcal{I}_d^I \times \mathcal{I}_d^I}$.
- Splitting of \mathbb{T} : $\mathbb{T} = \begin{pmatrix} \mathbb{T}_1 & 0 \\ 0 & \mathbb{T}_2 \end{pmatrix}$ with: $\mathbb{T}_I = (\mathbb{T})_{(k,l) \in \mathcal{I}_\phi^I \times \mathcal{I}_\phi^I}$. \mathbb{T}_I are symmetric positive-definite matrices.

Second, we split the current, the flux and the source vectors as well, so that:

- $\underline{\mathbf{p}}_x = \left(\overset{\circ}{\underline{\mathbf{p}}}_x^1, \underline{\mathbf{p}}_\Gamma, \overset{\circ}{\underline{\mathbf{p}}}_x^2 \right)^T$, with: $\overset{\circ}{\underline{\mathbf{p}}}_x^I = \left(\underline{\mathbf{p}}_x \right)_{k \in \mathcal{I}_x^I}$, $\underline{\mathbf{p}}_\Gamma = \left(\underline{\mathbf{p}}_x \right)_{k \in \mathcal{I}_\Gamma^I}$,
- $\underline{\mathbf{p}}_d = \left(\underline{\mathbf{p}}_d^1, \underline{\mathbf{p}}_d^2 \right)^T$, with: $\underline{\mathbf{p}}_d^I = \left(\underline{\mathbf{p}}_d \right)_{k \in \mathcal{I}_d^I}$,
- $\underline{\phi} = \left(\underline{\phi}_1, \underline{\phi}_2 \right)$, with: $\underline{\phi}_I = \left(\underline{\phi} \right)_{k \in \mathcal{I}_\phi^I}$,
- $\underline{\mathbf{S}}_f = \left(\underline{\mathbf{S}}_f^1, \underline{\mathbf{S}}_f^2 \right)$, with: $\underline{\mathbf{S}}_f^I = \left(\underline{\mathbf{S}}_f \right)_{k \in \mathcal{I}_\phi^I}$.

Let's duplicate $\underline{\mathbf{p}}_\Gamma$, setting $\underline{\mathbf{p}}_\Gamma = \underline{\mathbf{p}}_\Gamma^1 = \underline{\mathbf{p}}_\Gamma^2$.

Let $\beta^I \in \mathbb{R}^{N_\Gamma} \times \mathbb{R}^{N_\Gamma}$ be the diagonal matrices such that $\beta_{k,k}^I = \alpha_{I,k}^{-1}$, $\alpha_{I,k} > 0$. We can write the line $-\mathbb{A}_x \underline{\mathbf{p}}_x + \mathbb{B}_x \phi = 0$ of the block linear system (14) this way:

$$\begin{cases} -\overset{\circ}{\mathbb{A}}_x^I \overset{\circ}{\underline{\mathbf{p}}}_x^I - \left(\overset{\circ}{\mathbb{A}}_\Gamma^I \right)^T \underline{\mathbf{p}}_\Gamma^I + \overset{\circ}{\mathbb{B}}_x^I \underline{\phi}_I = 0, \\ -\overset{\circ}{\mathbb{A}}_\Gamma^I \overset{\circ}{\underline{\mathbf{p}}}_x^I - \left(\mathbb{A}_\Gamma^I + \beta_I \right) \underline{\mathbf{p}}_\Gamma^I + \mathbb{B}_\Gamma^I \underline{\phi}_I = \overset{\circ}{\mathbb{A}}_\Gamma^J \overset{\circ}{\underline{\mathbf{p}}}_x^J + \left(\mathbb{A}_\Gamma^J - \beta_I \right) \underline{\mathbf{p}}_\Gamma^J - \mathbb{B}_\Gamma^J \underline{\phi}_J. \end{cases}$$

Whereas the lines $-\mathbb{A}_d \underline{\mathbf{p}}_d + \mathbb{B}_d \phi = 0$ of (14) write: $-\mathbb{A}_d^I \underline{\mathbf{p}}_d^I + \mathbb{B}_d^I \phi_I = 0$.

Finally, the line $\mathbb{T} \phi + \mathbb{B}^T \underline{\mathbf{p}} = \underline{\mathbf{S}}_f$ of (14) writes:

$$\mathbb{T}_I \underline{\phi}_I + \left(\overset{\circ}{\mathbb{B}}_x^I \right)^T \overset{\circ}{\underline{\mathbf{p}}}_x^I + \left(\mathbb{B}_\Gamma^I \right)^T \underline{\mathbf{p}}_\Gamma^I + \left(\mathbb{B}_y^I \right)^T \underline{\mathbf{p}}_y^I = \underline{\mathbf{S}}_f^I.$$

Third, introduce:

- The matrices \mathbb{A}_{II} and \mathbb{A}_{IJ} :

$$\mathbb{A}_{II} = \begin{pmatrix} \overset{\circ}{\mathbb{A}}_x^I & \left(\overset{\circ}{\mathbb{A}}_\Gamma^I \right)^T & 0 \\ \overset{\circ}{\mathbb{A}}_\Gamma^I & \left(\mathbb{A}_\Gamma^I + \beta_I \right) & 0 \\ 0 & 0 & \mathbb{A}_y^I \end{pmatrix} \text{ and } \mathbb{A}_{IJ} = \begin{pmatrix} 0 & 0 & 0 \\ \overset{\circ}{\mathbb{A}}_\Gamma^J & \left(\mathbb{A}_\Gamma^J - \beta_I \right) & 0 \\ 0 & 0 & 0 \end{pmatrix}$$

\mathbb{A}_{II} are symmetric positive-definite matrices.

Remark 5. The terms $(\beta_I)_{I=1,2}$ play an important role: if either $\beta_1 = \beta_2 = 0$ (Dirichlet interface conditions) or $\beta_1 = \beta_2 \rightarrow +\infty$ (Neuman interface conditions), then the matrix $\begin{pmatrix} \mathbb{A}_{11} & \mathbb{A}_{12} \\ \mathbb{A}_{21} & \mathbb{A}_{22} \end{pmatrix}$ of the linear system stemming from the Schwarz iterative algorithm is either not invertible, or very ill-conditioned. On the other hand, in other cases, it stabilizes the linear system.

- The matrices \mathbb{B}_{II} , and \mathbb{B}_{IJ} :

$$\mathbb{B}_{II} = \begin{pmatrix} \mathring{\mathbb{B}}_x^I \\ \mathbb{B}_\Gamma^I \\ \mathbb{B}_y^I \end{pmatrix}, \mathbb{B}_{IJ} = \begin{pmatrix} 0 \\ \mathbb{B}_\Gamma^J \\ 0 \end{pmatrix}. \quad (32)$$

- The vectors $\underline{\mathbf{p}}_I = (\underline{\mathbf{p}}_x^I, \underline{\mathbf{p}}_y^I)^T$, with: $\underline{\mathbf{p}}_x^I = (\mathring{\underline{\mathbf{p}}}_x^I, \underline{\mathbf{p}}_\Gamma^I)^T$.

Finally, we can rewrite equivalently the linear system (14) of the discrete variational formulation as the linear systems below:

$$\begin{pmatrix} -\mathbb{A}_{II} & \mathbb{B}_{II} \\ \mathbb{B}_{II}^T & \mathbb{T}_I \end{pmatrix} \begin{pmatrix} \underline{\mathbf{p}}_I \\ \underline{\phi}_I \end{pmatrix} = \begin{pmatrix} \mathbb{A}_{IJ} \underline{\mathbf{p}}_J - \mathbb{B}_{IJ} \underline{\phi}_J \\ S_f^I \end{pmatrix}. \quad (33)$$

5.2.2. Schwarz iterative algorithms (31)

On the other hand, let's consider $\underline{\mathbf{P}}_I = (\underline{\mathbf{p}}_I, \underline{\phi}_I)^T$, and $\underline{\mathbf{Q}}_I = (0, \underline{\mathbf{S}}_f^I)^T$ and set:

$$\mathbb{H}_{II} = \begin{pmatrix} -\mathbb{A}_{II} & \mathbb{B}_{II} \\ \mathbb{B}_{II}^T & \mathbb{T}_I \end{pmatrix} \text{ and } \mathbb{H}_{IJ} = \begin{pmatrix} -\mathbb{A}_{IJ} & \mathbb{B}_{IJ} \\ 0 & 0 \end{pmatrix}.$$

The linear systems (33) read now: $\mathbb{H}_{II} \underline{\mathbf{P}}_I = \underline{\mathbf{Q}}_I - \mathbb{H}_{IJ} \underline{\mathbf{P}}_J$.

Classically, one can solve these systems iteratively by means of a block Jacobi, or a block Gauss-Seidel, method. Let's set $\underline{\mathbf{P}}_I^0 := (\underline{\mathbf{p}}_I^0, \underline{\phi}_I^0)$. The iterative resolution of (33) then writes:

for $n \in \mathbb{N}$, find $\underline{\mathbf{P}}_I^{n+1} := (\underline{\mathbf{p}}_I^{n+1}, \underline{\phi}_I^{n+1})$ such that:

$$\begin{aligned} \mathbb{H}_{11} \underline{\mathbf{P}}_1^{n+1} &= \underline{\mathbf{Q}}_1 - \mathbb{H}_{12} \underline{\mathbf{P}}_2^n, \\ \mathbb{H}_{22} \underline{\mathbf{P}}_2^{n+1} &= \underline{\mathbf{Q}}_2 - \mathbb{H}_{21} \underline{\mathbf{P}}_1^{n(+1)}. \end{aligned} \quad (34)$$

This linear system corresponds exactly to the discretization of the variational formulations of the Schwarz iterative algorithms (31): block Jacobi for the

additive algorithm, and block Gauss-Seidel for the multiplicative algorithm. Note that we solve iteratively each equation on $\underline{\mathbf{P}}_I^{n+1}$, using an alternating direction algorithm. Indeed, we recall that $\underline{\mathbf{P}}_I = \left(\underline{\mathbf{p}}_I, \phi_I \right)^T$, with $\underline{\mathbf{p}}_I = \left(\underline{\mathbf{p}}_x^I, \underline{\mathbf{p}}_y^I \right)^T$, so that each equation on $\underline{\mathbf{P}}_I^{n+1}$ corresponds to the block linear system (15). Finally, we remind that the solution of (34) is embedded into the inverse power iteration algorithm.

6. Numerical results and parallel implementation

6.1. The solver

To perform computations, we use some components of the APOLLO3^{®1} code, the latest neutronics code of CEA/DEN (Commissariat à l'Énergie Atomique et aux Énergies Alternatives, Direction de l'Énergie Nucléaire), developed in collaboration with EDF and AREVA [14]. In particular, we use the MINOS solver, one of the deterministic solvers, to compute numerically k_{eff} . More specifically, the MINOS solver [2, 17, 3, 19] is a 3D, SP_N solver on structured cartesian and hexagonal grids, which is based on the inverse power algorithm (5).

6.2. Presentation of the industrial case

The results presented here concern a pressurized water reactor core of capacity 900 MWe (3D PWR 900 MWe core). The cross sections that we use come from experimental results [21]. A diagram in the (x, y) -plane (a top view) of this reactor core is given on fig. 1(a). The fuel assemblies (yellow squares) are surrounded by water (in blue), which acts as both coolant and neutron moderator. The neutrons are reflected back by the core barrel (in red). By misuse of language, we will call the environment of the fuel area the reflector.

The geometry of the fuel assemblies is cartesian. There are 23 fuel assemblies of height 15.6 cm along the z axis (the total height of the fuel area is of size 360 cm). There are 157 fuel assemblies in the (x, y) -plane. A fuel assembly has a square (x, y) section of sidelength 21.6 cm.

On fig. 1(b), the (x, y) geometry of the core model is shown. The orange squares represent the reflector, the green (resp. purple) squares represent the UOX (resp. MOX) fuel assemblies. There are 16 (resp. 23) different kinds

of UOX (resp. MOX) assemblies.

Finally, the computational domain is of total size $367 \times 367 \times 400 \text{ cm}^3$. Indeed, to account for the fact that the reflector must surround the fuel (in particular above and below the assemblies), the fuel is actually put between heights 20 cm to 380 cm .

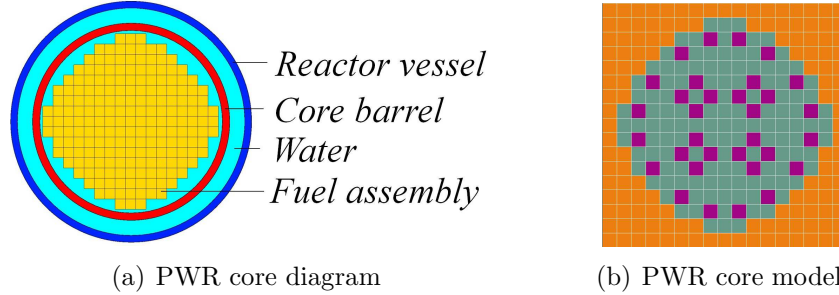


Figure 1: (x, y) core diagram and (x, y) core model of a 3D PWR 900MWe core.

On fig. 2(a), a diagram of the (x, y) -cut of an assembly is given. Each assembly is made of 289 (ie. 17×17) squared cells. A UOX (resp. MOX) assembly is made of cells containing either a cylindrical pin of UOX (resp. MOX) fuel, or a control rod; surrounded by water. Computationally, in each cell, the cross sections of the fuel (or the control rod) and the water are homogenized. Hence, their values can be very different from one cell to the other: in the present case, one ends up with 125 (resp. 32) cross section values for the UOX (resp. MOX) fuel. We have to solve a highly heterogeneous problem. On fig. 2(b) (resp. 2(c)), we give a model of the (x, y) -cut of a UOX (resp. MOX) assembly. The different colors correspond to different values of the homogenized cross sections (one value per cross section and per cell).

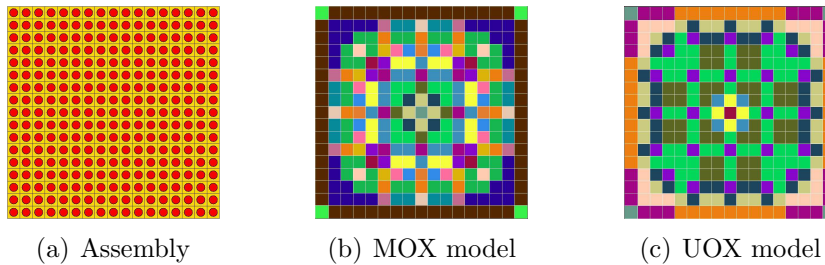


Figure 2: (x, y) assembly diagram; (x, y) MOX or UOX assembly model.

6.3. The algorithm

We perform a cell-by-cell computation, i.e. with one (x, y) unit mesh per assembly cell, on the diffusion approximation, with two energy groups. As already mentioned, in the inverse power algorithm, the outer iterations lead the convergence, so we can approximate the source solver by a single inner iteration: we end up with a single level of iteration (indexed by m). Now, compared with (20), we have an additional Gauss-Seidel iteration on the energy groups, so that the full algorithm reads:

Set $(\mathbf{p}_{g,I}^0, \phi_{g,I}^0)_{g,I}, k_{eff}^0, m = 0$.

Compute $S_{f,I}^0 = \sum_{g=1}^2 \Sigma_f^g \phi_{g,I}$.

Until convergence, do: $m \leftarrow m + 1$

For $g = 1, 2, g' = 2, 1$, do:

Solve:

$$\left\{ \begin{array}{l} \frac{1}{D_g} \mathbf{p}_{g,I}^{m+1} + \mathbf{grad} \phi_{g,I}^{m+1} = 0, \text{ in } \mathcal{R}_I, \\ \text{div } \mathbf{p}_{g,I}^{m+1} + \Sigma_a^g \phi_{g,I}^{m+1} = \frac{1}{k_{eff}^m} \chi^g S_{f,I}^m + \Sigma_{s,0}^{g' \rightarrow g} \phi_{g',I}^{m(+1)}, \text{ in } \mathcal{R}_I, \\ -\mathbf{p}_{g,I}^{m+1} \cdot \mathbf{n}_I + \alpha_{g,I} \phi_{g,I}^{m+1} = \mathbf{p}_{g,J}^{m(+1)} \cdot \mathbf{n}_J + \alpha_{g,I} \phi_{g,J}^{m(+1)}, \text{ on } \Gamma, \\ \phi_{g,I}^{m+1} = 0, \text{ on } \partial \mathcal{R} \cap \partial \mathcal{R}_I, \end{array} \right.$$

End

Compute $S_{f,I}^{m+1} = \sum_{g'=1}^2 \Sigma_f^{g'} \phi_{g',I}^{m+1}$.

Compute $k_{eff}^{m+1} = k_{eff}^m \frac{\sum_{I=1}^2 \int_{\mathcal{R}_I} (S_{f,I}^{m+1})^2}{2 \sum_{I=1}^2 \int_{\mathcal{R}_I} (S_{f,I}^{m+1} S_{f,I}^m)}$.

End

At iteration $m + 1$, the accuracy is measured on the fission source, expressed as a vector⁴ $\underline{\mathbf{S}}_f$:

$$\varepsilon_f^{m+1} = N_\phi \frac{\max_{i \in \mathcal{I}_\phi} |(\underline{\mathbf{S}}_f^{m+1} - \underline{\mathbf{S}}_f^m)_i|}{\sum_{i \in \mathcal{I}_\phi} |(\underline{\mathbf{S}}_f^{m+1})_i|},$$

The inverse power iteration algorithm is stopped when $\varepsilon_f^m < 10^{-5}$. The mesh is of size $289 \times 289 \times 60$ (≈ 5 M unit meshes): for each energy group, there are about 15M (resp. 5M) unknowns for the current (resp. the flux). The converged eigenvalue k_{eff} is 1.230157. For each group, we chose $\alpha_g = \sqrt{\Sigma_a^g D^g}$, with piecewise constant cross sections along the interfaces, which can be highly heterogeneous. Computations were carried out on the Titane computer, hosted by the CCRT (the CEA Supercomputing Center).

6.4. Numerical results

On Fig. 3, we report some resulting (x, y) normalized power distribution maps of these calculations. The normalized power distribution is defined by: $\underline{\mathcal{P}} = \mathcal{P} \frac{\int_{\mathcal{R}_F} 1}{\int_{\mathcal{R}_F} \mathcal{P}}$, where \mathcal{R}_F is the fuel volume, and \mathcal{P} is defined on each discrete

mesh R_m by: $\mathcal{P}(R_m) := \sum_g \kappa_m^g \int_{R_m} \phi^g$, κ_m^g being the energy released by

fission and capture for the group g in the mesh R_m . The green area represents the reflector where $\mathcal{P} = 0$. In the core (the place where fission occurs), the color coding runs from blue ($0 < \mathcal{P} \lesssim 1$) to white ($1 \lesssim \mathcal{P} \lesssim 1.4$) then red ($1.4 \lesssim \mathcal{P} \lesssim 3.7$). Note that it is only a shape representation, since we solve an eigenvalue problem.

In table 1, we present the results for computations of the MINOS solver from 1 to 128 computational cores with *RT0* finite elements. The data of table 1 is:

- N_c : The number of cores (ie. the number of subdomains).
- N_{DD} : The 3D Cartesian $(N_{DD}^x, N_{DD}^y, N_{DD}^z)$ decomposition.
- N_{out} : The number of outer iterations to achieve convergence.
- $Err.$: The (unsigned) difference between the computed and the converged eigenvalues, either sequentially or in parallel, times 10^{-5} .

⁴ $\underline{\mathbf{S}}_f$ is the discretization representation of the source $S_f := \sum_{g=1}^2 \Sigma_f^g \phi_g$.

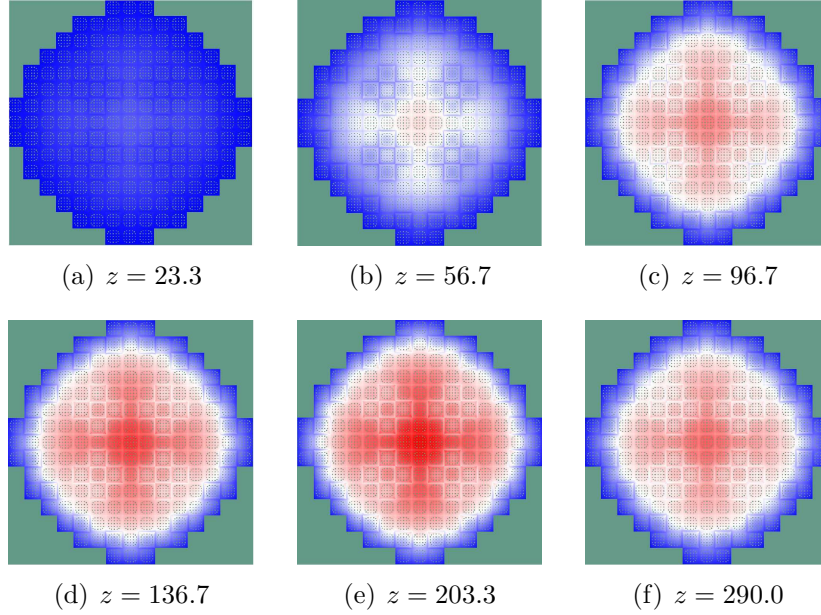


Figure 3: Power distribution maps of the neutron flux at different heights (in *cm*).

- *CPU*: The CPU time spent within the MINOS solver, given in seconds.
- *Eff.*: The efficiency (in %): namely, $T_1/(N_{DD} \times T_N)$, where T_1 (resp. T_N) is the total sequential (resp. parallel, on N_{DD} cores) CPU time.

As we can see, the method scales relatively well: its efficiency ranges from 67% to 88%. The number of outer iterations does not increase much, and accuracy is steady.

6.5. Influence of the partitioning

We consider the same computations as before, but we use a different splitting, along the z -axis only. We obtain the following results (table 2). As long as 32 or less cores are used, accuracy is steady and the number of outer iterations increases slowly. For 8 or more cores, the efficiency is worse than in Table 2. This is probably due to the fact that, with a splitting along the z -axis only, one increases the amount of transferred data. As a consequence the communication time also increases. Finally, for 48 or more cores, the accuracy deteriorates and the number of iterations grows: it seems better to divide the domain into several directions than along a single one only (in slices).

N_C	$N_{DD}(x, y, z)$	N_{out}	$Err. 10^{-5}$	$CPU (s)$	$Eff. (\%)$
1	(1, 1, 1)	380	0	284	100
2	(2, 1, 1)	380	0	166	85
4	(2, 2, 1)	379	0	105	67
8	(2, 2, 2)	377	0	53	67
16	(4, 4, 1)	377	0	25	71
32	(4, 4, 2)	385	0	10	88
64	(8, 8, 1)	393	0	5	88
128	(8, 8, 2)	393	0	2.6	85

Table 1: Computations results with the proposed numerical scheme.

N_C	$N_{DD}(x, y, z)$	N_{out}	$Err. 10^{-5}$	$CPU (s)$	$Eff. (\%)$
1	(1, 1, 1)	380	0	284	100
2	(1, 1, 2)	381	0	166	85
4	(1, 1, 4)	382	0	109	65
8	(1, 1, 8)	383	0	60	59
16	(1, 1, 16)	384	0	30	59
32	(1, 1, 32)	396	0	14	63
48	(1, 1, 48)	876	0.4	30	19
56	(1, 1, 56)	558	0.2	19	27

Table 2: Splitting along the z -axis.

Hence, one has to balance the transferred data versus the overall cost of the communications.

6.6. Influence of the α -parameter

In P. Guérin's PhD thesis [17], the α -parameter is tuned carefully. On the other hand, in S. Van Criekingen et al paper [38], the Schwarz iterative algorithm with Robin transmission conditions is applied to the P_N equations (discretized with non conforming finite elements). In which case, "*no theoretical result appears efficiently applicable*" [37] to optimize the α -parameter. We will see that in our case, the choice of the α -parameter has a great influence on the convergence.

In Section 4.5, we carried out some computations in order to optimize the

choice of α . Let's try other α -parameters. In the next computations, we are mainly interested in the accuracy and the number of outer iterations. In table 3 we give numerical results for $\alpha_g = 1$ and $\alpha_g = 0.5$ for both energy groups, with the same splittings as those reported in table 1.

Nc	$N_{DD}(x, y, z)$	$\alpha_g = 1$		$\alpha_g = 0.5$	
		N_{out}	$Errr. 10^{-5}$	N_{out}	$Errr. 10^{-5}$
1	(1, 1, 1)	380	0	380	0
2	(2, 1, 1)	462	0.2	621	0.4
4	(2, 2, 1)	501	0.2	756	0.3
8	(2, 2, 2)	558	0.2	931	0.4
16	(4, 4, 1)	549	0.2	891	0.3
32	(4, 4, 2)	622	0.2	1053	0.4
64	(8, 8, 1)	705	0.2	1184	0.4
128	(8, 8, 2)	790	0.3	1382	0.5

Table 3: Computations with $\alpha_g = 1$ and $\alpha_g = 0.5$.

In both cases, we note that the number of iterations increases faster than in table 1. Also, the accuracy is not as good as it is in table 1. Based on these experiments, it appears that the optimized choice of the α -parameter that we implemented is a good compromise, which in addition allows one to automate the method.

7. Conclusions

We analyzed a domain decomposition method based on the Schwarz iterative algorithm, to solve the mixed neutrons diffusion equations, from the continuous problem to its discretization with Raviart-Thomas finite elements. We developed an asymptotic method in order to optimize the choice of the α -parameter appearing in the interface conditions of Robin type. Numerical experiments carried out with the MINOS solver show that the method is robust and efficient both sequentially and in parallel, and that our choice of the α -parameter is satisfactory. Note that the number of iterations to solve our problem increases only slightly with the number of subdomains.

We believe we could improve the method along the following axes:

- We could use Ventcell interface conditions: in other words, enhancing the

efficiency of the Robin interface condition with the introduction of tangential derivatives [27, 20].

- We could compare our method with an overlapping domain decomposition method (ie. Dirichlet or Neumann interface conditions), with a coarse grid solver, as done in [28].

We also encoded the domain decomposition method for the SP_N equations with $N \geq 2$ on a cartesian mesh. In that case, the Robin interface conditions are written in a matricial form, the α -parameter becomes a square matrix, whose coefficients can be optimized as well [18].

Appendix A. Proof of Thm. 3

PROOF. According to Theorem 2, we already know that there exists a solution $(\mathbf{p}, \phi) \in \mathbf{Q} \times H_{0,\Gamma_D}^1(\mathcal{R})$ to (6), which in turns solves the variational formulation (10). Hence, we only have to establish uniqueness of the solution to (10) to conclude the proof. Classically, one looks for some inf-sup condition (for more details about the general framework, we refer to [6, 12]) to ensure uniqueness. For that, let us endow $\mathbf{Q} \times L^2(\mathcal{R})$ with the graph norm $|||(\mathbf{q}, \psi)||| = (\|\mathbf{q}\|_{\mathbf{Q}}^2 + \|\psi\|_0^2)^{1/2}$, and rewrite the variational formulation (10) – with obvious notations – as:

Find $(\mathbf{p}, \phi) \in \mathbf{Q} \times L^2(\mathcal{R})$ such that $\forall (\mathbf{q}, \psi) \in \mathbf{Q} \times L^2(\mathcal{R})$:

$$c((\mathbf{p}, \phi), (\mathbf{q}, \psi)) = \ell((\mathbf{q}, \psi)).$$

In this setting, the inf-sup condition writes

$$\exists \eta > 0, \quad \inf_{(\mathbf{p}, \phi) \in \mathbf{Q} \times L^2(\mathcal{R})} \sup_{(\mathbf{q}, \psi) \in \mathbf{Q} \times L^2(\mathcal{R})} \frac{c((\mathbf{p}, \phi), (\mathbf{q}, \psi))}{|||(\mathbf{p}, \phi)||| |||(\mathbf{q}, \psi)|||} \geq \eta.$$

Given $(\mathbf{p}, \phi) \in \mathbf{Q} \times L^2(\mathcal{R})$, let us consider the two cases below.

Assume first that $\operatorname{div} \mathbf{p} = 0$ in Ω , then

$$c((\mathbf{p}, \phi), (\mathbf{q}, \psi)) = \int_{\mathcal{R}} \left(-\frac{1}{D} \mathbf{p} \cdot \mathbf{q} + \phi \operatorname{div} \mathbf{q} + \Sigma_a \phi \psi \right) - \int_{\Gamma_R} \frac{1}{\alpha} (\mathbf{p} \cdot \mathbf{n})(\mathbf{q} \cdot \mathbf{n}).$$

By choosing $(\mathbf{q}, \psi) = (-\mathbf{p}, \phi) \in \mathbf{Q} \times L^2(\mathcal{R})$, one has $|||(\mathbf{q}, \psi)||| = |||(\mathbf{p}, \phi)|||$ and moreover the expression of $c((\mathbf{p}, \phi), (\mathbf{q}, \psi))$ involves only positive terms, which yields easily the bound in this divergence-free case:

$$c((\mathbf{p}, \phi), (\mathbf{q}, \psi)) = \int_{\mathcal{R}} \left(\frac{1}{D} |\mathbf{p}|^2 + \Sigma_a (\phi)^2 \right) + \int_{\Gamma_R} \frac{1}{\alpha} (\mathbf{p} \cdot \mathbf{n})^2$$

$$\begin{aligned}
&\geq \min((D^*)^{-1}, \alpha^{-1}) \|\mathbf{p}\|_{\mathbf{Q}}^2 + (\Sigma_a)_* \|\phi\|_0^2 \\
&\geq \min((D^*)^{-1}, \alpha^{-1}, (\Sigma_a)_*) \|\!(\mathbf{p}, \phi)\!\|^2 \\
&= \min((D^*)^{-1}, \alpha^{-1}, (\Sigma_a)_*) \|\!(\mathbf{p}, \phi)\!\| \|\!(\mathbf{q}, \psi)\!\|.
\end{aligned}$$

In the general case ($\operatorname{div} \mathbf{p} \neq 0$), one can still proceed along the same lines, as soon as the terms in $\phi \operatorname{div} \mathbf{p}$ cancel out. A possible choice is $(\mathbf{q}, \psi) = (-\mathbf{p}, \frac{1}{2}\phi + \frac{1}{2}(\Sigma_a)^{-1} \operatorname{div} \mathbf{p}) \in \mathbf{Q} \times L^2(\mathcal{R})$. Indeed, one obtains the bounds:

$$\begin{aligned}
\|\!(\mathbf{q}, \psi)\!\|^2 &\leq \|\mathbf{p}\|_{\mathbf{Q}}^2 + \frac{1}{2} \|\phi\|_0^2 + \frac{1}{2} \|(\Sigma_a)^{-1} \operatorname{div} \mathbf{p}\|_0^2 \\
&\leq \max(1 + \frac{1}{2}((\Sigma_a)_*)^{-2}, \frac{1}{2}) \|\!(\mathbf{p}, \phi)\!\|^2, \text{ and} \\
c((\mathbf{p}, \phi), (\mathbf{q}, \psi)) &= \int_{\mathcal{R}} \left(\frac{1}{D} |\mathbf{p}|^2 + \frac{1}{2\Sigma_a} (\operatorname{div} \mathbf{p})^2 + \frac{\Sigma_a}{2} (\phi)^2 \right) + \int_{\Gamma_R} \frac{1}{\alpha} (\mathbf{p} \cdot \mathbf{n})^2 \\
&\geq \min((D^*)^{-1}, (2(\Sigma_a)^*)^{-1}, \alpha^{-1}, \frac{(\Sigma_a)_*}{2}) \|\!(\mathbf{p}, \phi)\!\|^2.
\end{aligned}$$

This concludes the proof.

Appendix B. Proof of Thm. 4

PROOF. Proving the first result is classical, see for instance [34, 12]: one has to obtain a uniform (ie. independent of h) discrete inf-sup condition. To that aim, one applies the construction of Theorem 3 to the discrete case, using the consistency property of the finite element spaces \mathbf{Q}_h^k and V_h^k .

The improved convergence result can be found in [34] (see theorem 13.2, p. 582, and (6.19-6.20) pp. 553-554). It makes use of local estimates.

Appendix C. Proof of Eq. (17)

This proof will be useful to show Prop. 5 (Subsection 4.4). Consider *a priori* that the solutions to (6) and (16) are independent one from the others, and set $(\mathbf{e}_I, \varepsilon_I) = (\mathbf{p}_I, \phi_I) - (\mathbf{p}, \phi)|_{\mathcal{R}_I}$. These errors satisfy

$$\left\{ \begin{array}{ll} \frac{1}{D} \mathbf{e}_I + \mathbf{grad} \varepsilon_I = 0, & \text{in } \mathcal{R}_I, \\ \operatorname{div} \mathbf{e}_I + \Sigma_a \varepsilon_I = 0, & \text{in } \mathcal{R}_I, \\ \varepsilon_1 = \varepsilon_2, & \text{on } \Gamma, \\ -\mathbf{e}_1 \cdot \mathbf{n}_1 = \mathbf{e}_2 \cdot \mathbf{n}_2, & \text{on } \Gamma. \end{array} \right. \quad (\text{C.1})$$

Let us multiply the first (resp. second) equation by \mathbf{e}_I (resp. ε_I), and integrate over \mathcal{R}_I . We obtain that:

$$\begin{cases} \int_{\mathcal{R}_I} \frac{1}{D} |\mathbf{e}_I|^2 + \int_{\mathcal{R}_I} \mathbf{grad} \varepsilon_I \cdot \mathbf{e}_I = 0, \\ \int_{\mathcal{R}_I} \operatorname{div} \mathbf{e}_I \varepsilon_I + \int_{\mathcal{R}_I} \Sigma_a \varepsilon_I^2 = 0. \end{cases} \quad (\text{C.2})$$

Using Green's first identity (8) and the second equation of (C.2), the first equation of (C.2) becomes:

$$\int_{\mathcal{R}_I} \frac{1}{D} |\mathbf{e}_I|^2 + \int_{\mathcal{R}_I} \Sigma_a \varepsilon_I^2 + \langle \varepsilon_I, \mathbf{e}_I \rangle = 0, \quad (\text{C.3})$$

where $\mathbf{e}_I = \mathbf{e}_I \cdot \mathbf{n}_{I|\Gamma}$. We sum the two equations over \mathcal{R}_1 and \mathcal{R}_2 :

$$\begin{aligned} \sum_{I=1}^2 \int_{\mathcal{R}_I} \frac{1}{D} |\mathbf{e}_I|^2 + \int_{\mathcal{R}_I} \Sigma_a \varepsilon_I^2 &= - \sum_{I=1}^2 \langle \varepsilon_I, \mathbf{e}_I \rangle, \\ &= - \langle \varepsilon_1, \mathbf{e}_1 + \mathbf{e}_2 \rangle, \text{ since } \varepsilon_1 = \varepsilon_2, \\ &= 0, \text{ since } \mathbf{e}_1 = -\mathbf{e}_2. \end{aligned}$$

Under the assumptions on D and Σ_a , we conclude that $\mathbf{e}_I = \mathbf{0}$ in $L^2(\mathcal{R}_I)^d$ and $\varepsilon_I = 0$ in $L^2(\mathcal{R}_I)$. Thanks to the first two equations in (C.1), this is also true in $\mathbf{H}(\operatorname{div}, \mathcal{R}_I) \times H^1(\mathcal{R}_I)$. In other words, we have that the solutions to (6) and (16) necessarily coincide, that is $(\mathbf{p}_I, \phi_I) = (\mathbf{p}, \phi)|_{\mathcal{R}_I}$ in $\mathbf{H}(\operatorname{div}, \mathcal{R}_I) \times H^1(\mathcal{R}_I)$.

Appendix D. Proof of Prop. 5

PROOF. We will proceed as in Subsection 4.2 and use similar notations to compute the errors between two successive iterations. Note that as $\mathbf{p}^0 \cdot \mathbf{n}_{|\Gamma} \in L^2(\Gamma)$, it follows easily by induction in (19) that $\mathbf{p}^{n+1} \cdot \mathbf{n}_{|\Gamma} \in L^2(\Gamma)$, $\forall n \in \mathbb{N}$. As $\mathbf{p} \cdot \mathbf{n}_{|\Gamma} \in L^2(\Gamma)$, there holds $\varepsilon_I^{n+1} \in L^2(\Gamma)$, $\forall n \in \mathbb{N}$, so brackets can be replaced by integrals over the interface. Then, the errors satisfy, $\forall n \in \mathbb{N}^*$:

$$\int_{\mathcal{R}_I} \frac{1}{D} |\mathbf{e}_I^{n+1}|^2 + \int_{\mathcal{R}_I} \Sigma_a |\varepsilon_I^{n+1}|^2 + \int_{\Gamma} \mathbf{e}_I^{n+1} \varepsilon_I^{n+1} = 0. \quad (\text{D.1})$$

We sum the equations (D.1) over the two domains:

$$\sum_{I=1}^2 \left(\int_{\mathcal{R}_I} \frac{1}{D} |\mathbf{e}_I^{n+1}|^2 + \int_{\mathcal{R}_I} \Sigma_a |\varepsilon_I^{n+1}|^2 \right) + \sum_{I=1}^2 \int_{\Gamma} \mathbf{e}_I^{n+1} \varepsilon_I^{n+1} = 0. \quad (\text{D.2})$$

We use the identity: $AB = \frac{1}{4\alpha} ((A + \alpha B)^2 - (-A + \alpha B)^2)$, so that:

$$\begin{aligned} \int_{\Gamma} e_1^{n+1} \varepsilon_1^{n+1} &= \frac{1}{4\alpha} \int_{\Gamma} ((e_1^{n+1} + \alpha \varepsilon_1^{n+1})^2 - (-e_1^{n+1} + \alpha \varepsilon_1^{n+1})^2), \\ \int_{\Gamma} e_2^{n+1} \varepsilon_2^{n+1} &= \frac{1}{4\alpha} \int_{\Gamma} ((e_2^{n+1} + \alpha \varepsilon_2^{n+1})^2 - (-e_2^{n+1} + \alpha \varepsilon_2^{n+1})^2), \\ &= \frac{1}{4\alpha} \int_{\Gamma} ((-e_1^{n+2} + \alpha \varepsilon_1^{n+2})^2 - (e_1^{n(+1)} + \alpha \varepsilon_1^{n(+1)})^2). \end{aligned} \tag{D.3}$$

For the last equality, we used the interface conditions in (18) and (19), whose differences yield respectively

$$\begin{cases} -e_1^{n+2} + \alpha \varepsilon_1^{n+2} &= e_2^{n+1} + \alpha \varepsilon_2^{n+1} \text{ on } \Gamma, \\ -e_2^{n+1} + \alpha \varepsilon_2^{n+1} &= e_1^{n(+1)} + \alpha \varepsilon_1^{n(+1)} \text{ on } \Gamma, \end{cases}$$

Equation (D.2) writes now in the case of the MSM:

$$\begin{aligned} &\sum_{I=1}^2 \left(\int_{\mathcal{R}_I} \frac{1}{D} |\mathbf{e}_I^{n+1}|^2 + \int_{\mathcal{R}_I} \Sigma_a |\varepsilon_I^{n+1}|^2 \right) \\ &+ \frac{1}{4\alpha} \int_{\Gamma} [(-e_1^{n+2} + \alpha \varepsilon_1^{n+2})^2 - (-e_1^{n+1} + \alpha \varepsilon_1^{n+1})^2] = 0 \end{aligned} \tag{D.4}$$

In the case of the ASM, we have two more terms:

$$\begin{aligned} &\sum_{I=1}^2 \left(\int_{\mathcal{R}_I} \frac{1}{D} |\mathbf{e}_I^{n+1}|^2 + \int_{\mathcal{R}_I} \Sigma_a |\varepsilon_I^{n+1}|^2 \right) \\ &+ \frac{1}{4\alpha} \int_{\Gamma} [(-e_1^{n+2} + \alpha \varepsilon_1^{n+2})^2 - (-e_1^{n+1} + \alpha \varepsilon_1^{n+1})^2] \\ &+ \frac{1}{4\alpha} \int_{\Gamma} [(e_1^{n+1} + \alpha \varepsilon_1^{n+1})^2 - (e_1^n + \alpha \varepsilon_1^n)^2] = 0 \end{aligned} \tag{D.5}$$

When we sum these norms of errors from $n = 0$ to N , the boundary terms cancel each other out but the first and the last terms. We have for the MSM:

$$\begin{aligned} &\sum_{n=0}^N \left\{ \sum_{I=1}^2 \left(\int_{\mathcal{R}_I} \frac{1}{D} |\mathbf{e}_I^{n+1}|^2 + \int_{\mathcal{R}_I} \Sigma_a |\varepsilon_I^{n+1}|^2 \right) \right\} \\ &+ \frac{1}{4\alpha} \int_{\Gamma} (-e_1^{N+2} + \alpha \varepsilon_1^{N+2})^2 = \frac{1}{4\alpha} \int_{\Gamma} (-e_1^1 + \alpha \varepsilon_1^1)^2. \end{aligned} \tag{D.6}$$

In the case of the ASM, we obtain two more terms:

$$\begin{aligned}
& \sum_{n=0}^N \left\{ \sum_{I=1}^2 \left(\int_{\mathcal{R}_I} \frac{1}{D} |\mathbf{e}_I^{n+1}|^2 + \int_{\mathcal{R}_I} \Sigma_a |\varepsilon_I^{n+1}|^2 \right) \right\} \\
& + \frac{1}{4\alpha} \int_{\Gamma} [(-e_1^{N+2} + \alpha\varepsilon_1^{N+2})^2 + (e_1^{N+1} + \alpha\varepsilon_1^{N+1})^2] = \quad (\text{D.7}) \\
& \frac{1}{4\alpha} \int_{\Gamma} [(-e_1^1 + \alpha\varepsilon_1^1)^2 + (e_1^0 + \alpha\varepsilon_1^0)^2].
\end{aligned}$$

We conclude that the series

$$\sum_{n=0}^{\infty} \left\{ \sum_{I=1}^2 \left(\int_{\mathcal{R}_I} \frac{1}{D} |\mathbf{e}_I^n|^2 + \int_{\mathcal{R}_I} \Sigma_a |\varepsilon_I^n|^2 \right) \right\}$$

are convergent. Moreover, under the assumptions on D and Σ_a , the sequences $(\mathbf{e}_I^n, \varepsilon_I^n)_n$ tend to zero in $L^2(\mathcal{R}_I)^d \times L^2(\mathcal{R}_I)$. Going back to the first two equations of (C.1) written here with unknowns $(\mathbf{e}_I^n, \varepsilon_I^n)$, we conclude that the sequences $(\mathbf{e}_I^n, \varepsilon_I^n)$ converge to zero in $\mathbf{H}(\text{div}, \mathcal{R}_I) \times H^1(\mathcal{R}_I)$.

References

- [1] M. Barrault, B. Lathuilière, P. Ramet, and J. Roman. Efficient parallel resolution of the simplified transport equations in mixed-dual formulation. J. Comput. Phys., 230:2004–2020, 2011.
- [2] A.-M. Baudron and J.-J. Lautard. MINOS: A Simplified P_N solver for core calculations. Nuclear Science and Engineering, 155:250–263, 2007.
- [3] A.-M. Baudron and J.-J. Lautard. SP_N core calculations in the APOLLO3 System. In Mathematics and Computational Methods Applied to Nuclear Science and Engineering (M&C 2011). Latin American Section (LAS) / American Nuclear Society (ANS), 2011.
- [4] F. Ben Belgacem, C. Bernardi, M. Costabel, and M. Dauge. Un résultat de densité pour les équations de Maxwell. C. R. Acad. Sci. Paris, Ser. I, 324:731–736, 1997.
- [5] F. Ben Belgacem, C. Bernardi, and F. Rapetti. Numerical analysis of a model for an axisymmetric guide for electromagnetic waves. Part I: The Fourier analysis. Math. Meth. Appl. Sci., 28:2007–2029, 2005.
- [6] F. Brezzi and M. Fortin. Mixed and hybrid finite element methods. Springer-Verlag, 1991.
- [7] J. Bussac and P. Reuss. Traité de neutronique. Hermann, 1985.
- [8] G. Cossa, V. Giusti, and B. Montagnini. A boundary element-response matrix method for criticality diffusion problems in xyz geometry. Annals of Nuclear Energy, 37:953–973, 2010.
- [9] F. Coulomb. Domain decomposition and mixed finite elements for the neutron diffusion equation. In T.F. Chan et al., editors, Second International Symposium on Domain Decomposition Methods for Partial Differential Equations, pages 295–313. SIAM, 1989.
- [10] F. Coulomb and C. Fedon-Magnaud. Mixed and mixed hybrid elements for the diffusion equation. Nuclear Science and Engineering, 100(3):218–225, 1988.
- [11] J. J. Duderstadt and L. J. Hamilton. Nuclear reactor analysis. John Wiley & Sons, Inc., 1976.

- [12] A. Ern and J.-L. Guermond. Theory and practice of finite elements. Springer-Verlag, 2004.
- [13] M. Gander. Optimized Schwarz methods. SIAM J. Numer. Anal., 44(2):699–731, 2006.
- [14] H. Golfier, R. Lenain, J.-J. Lautard, Ph. Fougeras, Ph. Magat, E. Martinoli, and Y. Duteillet. APOLLO3: a common project of CEA, AREVA and EDF for the development of a new deterministic multi-purpose code for core physics analysis. In International Conference on Advances in Mathematics, Computational Methods, and Reactor Physics (M&C 2009). American Nuclear Society (ANS), 2009.
- [15] P. Grisvard. Elliptic problems in nonsmooth domains. Pitman, 1985.
- [16] P. Grisvard. Singularities in boundary value problems, volume 22 of RMA. Masson, 1992.
- [17] P. Gu erin. M ethodes de d ecomposition de domaine pour la formulation mixte duale du probl eme critique de la diffusion des neutrons. PhD thesis, Universit e Pierre et Marie Curie, Paris (In French), 2007.
- [18] E. Jamelot, A.-M. Baudron, and J.-J. Lautard. Domain decomposition for the SP_N solver MINOS. Transport Theory and Statistical Physics, [To appear, 2013](#).
- [19] E. Jamelot, J. Dubois, J.-J. Lautard, A.-M. Baudron, and C. Calvin. High performance 3D neutron transport on petascale and hybrid architectures within APOLLO3 code. In International Conference on Mathematics and Computational Methods Applied to Nuclear Science and Engineering (M&C 2011). Latin American Section (LAS) / American Nuclear Society (ANS), 2011.
- [20] C. Japhet, F. Nataf, and F. Rogier. The optimized order 2 method: application to convection diffusion problems. Future Generation Computer Systems, 18(1):18–30, 2001.
- [21] J. Krebs, M.-C. Laigle, R. Lenain, G. Mathonni ere, and A. Nicolas. Calculational methods for PWR. In Specialist Meeting on Advanced Calculational Methods for Power Reactors, Cadarache, France. International Atomic Energy Agency, 1990.

- [22] M. G. Krein and M. A. Rutman. Amer. Math. Soc. Translation, 1950.
- [23] B. Lathuilière. Méthodes de décomposition de domaine pour les équations du transport simplifié en neutronique. PhD thesis, Université de Bordeaux I (In French), 2010.
- [24] P.-L. Lions. On the Schwarz alternating method I. In R. Glowinski et al., editors, First International Symposium on Domain Decomposition Methods for Partial Differential equations, pages 1–42. SIAM, 1988.
- [25] P.-L. Lions. On the Schwarz alternating method III: a variant for nonoverlapping subdomains. In T. F. Chan et al., editors, Third International Symposium Domain Decomposition Methods for Partial Differential equations, pages 202–223. SIAM, 1990.
- [26] H. Nakata and W. R. Martin. The finite element matrix method. Nucl. Sci. Eng., 85:289–305, 1983.
- [27] F. Nataf and F. Nier. Convergence rate of some domain decomposition methods for overlapping and nonoverlapping subdomains. Numer. Math., 75:357–377, 1997.
- [28] F. Nataf, H. Xiang, and V. Dolean. A two level domain decomposition preconditioner based on local Dirichlet-to-Neumann maps. C. R. Acad. Sci. Paris, Ser. I, 348:1163–1167, 2010.
- [29] J.-C. Nédélec. A new family of mixed finite elements in \mathbb{R}^3 . Numer. Math., 50:57–81, 1986.
- [30] G. J. Pomraning. Asymptotic and variational derivations of the simplified P_N equations. Annals of Nuclear Energy, 20(9):623–637, 1993.
- [31] A. Quarteroni and A. Valli. Domain decomposition methods for partial differential equations. Oxford Science Publications, 1999.
- [32] J. A. Rathkopf and W. R. Martin. The finite response matrix method for the solution of the neutron transport equation. Progress in Nuclear Energy, 18(1/2):237–250, 1986.
- [33] P.-A. Raviart and J.-M. Thomas. A mixed finite element method for second order elliptic problems. In Mathematical aspects of finite element

- methods, volume 606 of Lecture Notes in Mathematics, pages 292–315. Springer, 1977.
- [34] J. E. Roberts and J.-M. Thomas. Mixed and hybrid methods. In P. G. Ciarlet and J.-L. Lions, editors, Handbook of Numerical Analysis. Volume II, pages 523–629. North Holland, 1991.
- [35] D. Schneider. Eléments finis mixtes duaux pour la résolution numérique de l'équation de la diffusion neutronique en géométrie hexagonale. PhD thesis, Université Pierre et Marie Curie, Paris (In French), 2000.
- [36] H. A. Schwarz. Uber einige Abbildungsaufgaben. Ges. Math Abh., 11:65–83, 1869.
- [37] S. Van Criekingen. Domain decomposition P_N solutions to the 3D transport benchmark over a range in parameter space. In Advances in Reactor Physics Linking Research, Industry, and Education (Physor 2012). American Nuclear Society (ANS), 2012.
- [38] S. Van Criekingen, F. Nataf, and P. Havé. PARAFISH: a parallel FE- P_N neutron transport solver based on domain decomposition. Annals of Nuclear Energy, 38(1):145–150, 2011.
- [39] L. Y. Zaslavsky. An adaptative algebraic multigrid for multigroup neutron diffusion reactor core calculations. Appl. Math. Comput., 53:13–26, 1993.
- [40] L. Y. Zaslavsky. An adaptative algebraic multigrid for reactor criticality calculations. SIAM J. Sci. Comput., 16(4):840–847, 1995.